International Ocean Discovery Program
Expedition 359 Scientific Prospectus

Sea Level, Currents, and Monsoon Evolution in the Indian Ocean

Christian Betzler
Co-Chief Scientist
Centrum für Erdsystemforschung und Nachhaltigkeit
Institut für Geologie
University of Hamburg
20146 Hamburg
Germany

Gregor P. Eberli
Co-Chief Scientist
Division of Marine Geology and Geophysics
Rosenstiel School of Marine & Atmospheric Science
University of Miami
Miami FL 33149
USA

Liviu Giosan
Ancillary Project APL-849 Proponent
Woods Hole Oceanographic Institution
Woods Hole MA 02543
USA

Carlos A. Alvarez Zarikian
Expedition Project Manager/Staff Scientist
International Ocean Discovery Program
Texas A&M University
1000 Discovery Drive
College Station TX 77845
USA

Published by
International Ocean Discovery Program

Publisher's notes

This publication was prepared by the *JOIDES Resolution* Science Operator (JRSO) at Texas A&M University as an account of work performed under the International Ocean Discovery Program (IODP). Funding for the program is provided by the following agencies:

National Science Foundation (NSF), United States

Ministry of Education, Culture, Sports, Science and Technology (MEXT), Japan

European Consortium for Ocean Research Drilling (ECORD)

Ministry of Science and Technology (MOST), People's Republic of China

Korea Institute of Geoscience and Mineral Resources (KIGAM)

Australian Research Council (ARC) and GNS Science (New Zealand), Australian/New Zealand Consortium (ANZIC)

Ministry of Earth Sciences (MoES), India

Coordination for Improvement of Higher Education Personnel, Brazil

Disclaimer

This IODP *Scientific Prospectus* is based on precruise Science Advisory Structure panel discussions and scientific input from the designated Co-Chief Scientists on behalf of the drilling proponents. During the course of the cruise, actual site operations may indicate to the Co-Chief Scientists, the Staff Scientist/Expedition Project Manager, and the Operations Superintendent that it would be scientifically or operationally advantageous to amend the plan detailed in this prospectus. It should be understood that any proposed changes to the science deliverables outlined in the plan presented here are contingent upon the approval of the JRSO Science Services Director.

Copyright

Citation:
Betzler, C., Eberli, G.P., Giosan, L., and Alvarez Zarikian, C.A., 2014. Sea level, currents, and monsoon evolution in the Indian Ocean. *International Ocean Discovery Program Scientific Prospectus,* 359. http://dx.doi.org/10.14379/iodp.sp.359.2014

ISSN

World Wide Web: 2332-1385

November 2014

Abstract

International Ocean Discovery Program (IODP) Expedition 359 is designed to address sea level, currents, and monsoon evolution in the Indian Ocean. Seven proposed drill sites are located in the Maldives and one site is located in the Kerala-Konkan Basin on the western Indian continental margin. The Maldives carbonate edifice bears a unique and mostly unread Indian Ocean archive of the evolving Cenozoic icehouse world. It has great potential to serve as a key area for better understanding the effects of this global evolution in the Indo-Pacific realm. Based mainly on seismic stratigraphic data, a model for the evolution of this carbonate bank has been developed, showing how changing sea level and ocean current patterns shaped the bank geometries. A dramatic shift in development of the carbonate edifice from a sea level–controlled to a predominantly current-controlled system is thought to be directly linked to the evolving Indian monsoon. Fluctuations in relative sea level control the stacking pattern of depositional sequences during the lower to middle Miocene. This phase was followed by a two-fold configuration of bank development: bank growth continued in some parts of the edifice, whereas in other places, banks drowned. Drowning steps seem to coincide with onset and intensification of the monsoon-related current system and the deposition of giant sediment drifts. The shapes of drowned banks attest to the occurrence of these strong currents. The drift sediments, characterized by off-lapping geometries, formed large-scale prograding complexes, filling the Maldives Inner Sea basin. Because the strong current swept most of the sediment around the atolls away, relict banks did not prograde, and steady subsidence was balanced by aggradation of the atolls, which are still active today.

One important outcome of Expedition 359 is ground-truthing the hypothesis that the dramatic, pronounced change in the style of the sedimentary carbonate sequence stacking was caused by a combination of relative sea level fluctuations and ocean current system changes. Answering this question will directly improve our knowledge on processes shaping carbonate platforms and their stratigraphic records. Our findings would be clearly applicable to other Tertiary carbonate platforms in the Indo-Pacific region and to numerous others throughout the geological record. In addition, the targeted successions will allow calibration of the Neogene oceanic ^{13}C record with data from a carbonate platform to platform-margin series. This is becoming important, as such records are the only type that exist in deep time. Drilling will provide the cores required for reconstructing changing current systems through time that are directly related to the evolution of the Indian monsoon. As such, the drift deposits will provide a continuous record of Indian monsoon development in the region of the Mal-

dives. These data will be valuable for a comparison with proposed Site KK-03B in the Kerala-Konkan Basin (see **Geological setting of the Kerala-Konkan Basin,** below) and other monsoon-dedicated IODP expeditions.

The proposed site in the Kerala-Konkan Basin provides the opportunity to recover co-located oceanic and terrestrial records for monsoon and premonsoon Cenozoic climate in the eastern Arabian Sea and India, respectively. The site is located on a bathymetric high immediately north of the Chagos-Laccadive Ridge and is therefore not affected by strong tectonic, glacial, and nonmonsoon climatic processes that affect fan sites fed by Himalayan rivers. The cores are expected to consist of a continuous sequence of foraminifer-rich pelagic sediments with subordinate cyclical siliciclastic inputs of fluvial origin from the Indian Peninsula for the Neogene and a continuous paleoclimate record at orbital timescales into the Eocene and possibly the Paleocene.

Schedule for Expedition 359

Expedition 359 is based on International Ocean Discovery Program (IODP) drilling proposal 820-Full and Ancillary Proposal Letter-849 (available at **www.iodp.org/active-proposals**). Following ranking by the IODP Scientific Advisory Structure, the expedition was scheduled for the research vessel *JOIDES Resolution*, operating under contract with the *JOIDES Resolution* Science Operator (JRSO). At the time of publication of this *Scientific Prospectus*, the expedition is scheduled to start in Darwin, Australia, on 30 September 2015 and to end in Colombo, Sri Lanka, on 30 November 2015. A total of 61 days will be available for the drilling, coring, and downhole measurements described in this report (for the current detailed schedule, see **iodp.tamu.edu/scienceops**). Further details about the facilities aboard the *JOIDES Resolution* can be found at **www.iodp.tamu.edu/publicinfo/drillship.html.**

Introduction

Changes in oceanic circulation, sea level changes, and onset and fluctuations of the Indian monsoon characterize the Neogene. Located in the Indian Ocean, the Maldives carbonate edifice bears a record of these paleoclimatic changes. The archipelago, which rests on a volcanic basement ridge, is characterized by a double row of atolls encompassing a basin connected to the open ocean through passages. This basin, since the partial drowning of parts of the carbonate platform during the middle Miocene, serves as a depositional center of current-controlled deposits (drifts). This sedimentary system of drowned platform parts and drifts is the target of IODP Expedition 359, which aims to reconstruct its paleoceanographic evolution over the past 23 My.

Expedition 359 is designed to recover a series of neritic and hemipelagic deposits for the reconstruction of changes affecting the shallow-water carbonate factory of the edifice but also of the fluctuations in the ocean currents, which probably triggered this evolution. This reconstruction will be achieved by drilling 7 holes aligned into 2 transects covering shallow to deep-water deposits. The expedition builds on a series of seismic data sets that image the different steps of carbonate platform evolution and of previously drilled Ocean Drilling Program (ODP) Site 716.

More than 1200 km north of the Maldives sites (Figure **F1**), proposed Site KK-03B will be drilled on the western continental margin of India. Similar to the Maldives, the oceanographic conditions are dominated by the monsoon but with enhanced precipitation and continental freshwater influx due to orographic rain along the Western Ghats range that borders the western coast of India. Drilling is expected to recover a continuous sedimentary sequence containing a combined record of paleoclimate in peninsular India and an oceanic record of sea surface and intermediate water masses into the Eocene and possibly Paleocene.

Background

Geological setting of the Maldives

The Maldives archipelago in the central equatorial Indian Ocean is an isolated tropical carbonate platform constituting the central and largest part of the Chagos-Laccadives Ridge, which is located southwest of India (Figure **F1**). A north-south–oriented double row of atolls encloses the Inner Sea of the Maldives (Figure **F2**). The atolls are separated from each other by interatoll channels, which deepen toward the Indian Ocean (Purdy and Bertram, 1993). The Inner Sea is a bank-internal basin with water as deep as 550 m. The Maldives carbonate sedimentary succession is almost 3 km thick; it accumulated since the Eocene, away from any terrigenous input (Aubert and Droxler, 1992; Purdy and Bertram, 1993).

The archipelago comprises about 1200 smaller atolls, lying near or slightly above the sea surface. Discontinuous marginal rims formed by such small atolls surround lagoons with water depths up to 50–60 m. These rims are interrupted by deep passages, allowing strong currents within the atoll lagoons that rework and redeposit sediment and influence the growth of patch reefs (Ciarapica and Passeri, 1993). Modern marginal reefs are composed of robust-branching corals and coralline algae, whereas the lagoonal reefs show domal corals and detrital sand and rubble facies (Gischler et al., 2008). Muddy sediments are present only in the smaller atolls' lagoons protected by a continuous marginal reef rim (Ciarapica and Passeri, 1993; Gischler, 2006).

The oceanward margins of the Maldives archipelago are generally steeply inclined, with dips of 20°–30° to 2000 m water depth. On the Inner Sea side, stepped atoll slopes have the same dip angles but reach to water depths of only 150 m, where the gradient rapidly declines (Fürstenau et al., 2010). The Inner Sea is characterized by periplatform ooze deposition (Droxler et al., 1990; Malone et al., 1990), locally accumulated into sediment drift bodies (Betzler et al., 2009).

The climate and oceanographic setting of the Maldives is dictated by the seasonally reversing Indian monsoon system (Tomczak and Godfrey, 2003). Southwestern winds prevail during Northern Hemisphere summer (April–November), and northeastern winds prevail during winter (December–March). Winds generate ocean currents, which are directed westward in the winter and eastward in the summer. Interseasonally, a band of Indian Ocean equatorial westerlies establish, enforcing strong, eastward-flowing surface currents with velocities up to 1.3 m/s. Currents reach water depths of 200 m and more with only slightly reduced velocities (Tomczak and Godfrey, 2003). Within the modern atolls' passages, currents can exhibit velocities up to 2 m/s at the surface (Preu and Engelbrecht, 1991), accounting for winnowing in the passages and lagoons, where hard bottoms form (Ciarapica and Passeri, 1993; Gischler, 2006).

The Maldives formed on lower Paleogene (60–50 Ma) volcanic basement (Duncan and Hargraves, 1990). The long-term subsidence rate of the Maldives is roughly 0.03–0.04 mm/y based on deep core data from Well ARI-1 (Figure **F3**) (Aubert and Droxler, 1996; Belopolsky and Droxler, 2004a). In contrast, sedimentological data from the Rasdhoo atoll indicate a maximum subsidence rate of 0.15 mm/y during the past 135,000 y (Gischler et al., 2008). Faulting of the Maldives archipelago is reported to be restricted to pre-Miocene times (Purdy and Bertram, 1993). Stratigraphic data for the chronostratigraphic framework for seismic interpretation are derived from data from Wells NMA-1 and ARI-1 and Site 716 and are described by Purdy and Bertram (1993), Aubert and Droxler (1996), Belopolsky and Droxler (2004a), and Rio et al. (1990). Carbonate lithofacies, paleobathymetric evaluations, and biostratigraphic age determinations are based on cuttings and sidewall core analyses for Shell exploration Well ARI-1 first published by Aubert and Droxler (1996). A vertical seismic profile is used for time-depth conversion and to tie well data to seismic data (Figure **F3**, lower panel). For Site 716, which is covered by two high-resolution seismic lines (Figure **F4**), a simple time-depth estimation is made based on existing whole-core *P*-wave velocity measurements.

The Maldives comprise an approximately 3 km thick shallow-water carbonate succession (Belopolsky and Droxler, 2004a). Carbonate production established during the early Eocene when flat-topped carbonate banks began to form on topographic highs created by the volcanic basement during the Eocene to early Oligocene. During the late Oligocene, bank margins typically had elevated rims, which separated bank-interior areas from the open ocean. During the early Miocene, these banks partially drowned and carbonate production became restricted to narrow bands at the respective most oceanward areas. During the Miocene, bank margins prograded toward the Inner Sea, as recognized in different versions of reflection seismic data, irrespective of seismic resolution; however, details of the interpretation differ (Purdy and Bertram, 1993; Aubert and Droxler, 1996; Belopolsky and Droxler, 2004a). Aubert and Droxler (1996) differentiated the prograding margins into 4 Neogene units (N2–N5), with Unit N2 comprising the main phase of bank-margin progradation (Figure **F4**). Units N3–N5 were seen as its waning stage, with Unit N3 sediments interpreted as tending to be preferentially accumulated in front of the prograding bank margins. Unit N3 isochrons reveal that this unit is locally linked to areas of bank-margin disintegration, which in turn are associated with partial drowning and channel erosion (Aubert and Droxler, 1996). New higher resolution data prompted reinterpretation of the Units N3–N5 as large drift sequences. During the upper Miocene and Pliocene, the Inner Sea basin was filled while bank margins dominantly aggraded (Belopolsky and Droxler, 2004a) but also showed further partial drowning after Unit N5 deposition (Aubert and Droxler, 1996).

In the new high-resolution multichannel seismic data, 10 sequences are recognized in the lower and middle Miocene strata of the Maldives. They are interpreted to have formed in response to sea level–driven accommodation space variations (Betzler et al., 2013a) (Figure **F4C**). Platform Sequences (PS) 1–6 show development from a shallow ramp to a steep-flanked, reef-rimmed carbonate platform. Bank-edge reefs protect the lagoon, where back-reef aprons occur. At the PS6–PS7 transition, a switch from dominantly aggrading to dominantly prograding bank margins occurs. PS7–PS10 are composed of deposits formed in response to forced regression overlain by deposits formed during reflooding of the bank margins. These sequences lack bank-edge reefs, similar to other carbonate platforms of the Indo-Pacific realm, where community replacement in a neritic environment occurred (Halfar and Mutti, 2005; Betzler et al., 2013a).

Neogene sequences of the Maldives: middle Miocene to Pleistocene

The upper middle Miocene is characterized by the appearance of large-scale lobate clinoform bodies, attesting the onset of current amplification (Figures F4, F5, F6) in the Inner Sea (Betzler et al., 2013a; Lüdmann et al., 2013). These bodies are attached to passages where parts of barrier reefs drowned while relict banks and atolls grew elsewhere (Betzler et al., 2009, 2013a). Lobes are interpreted as "mega spillovers" fed by easterly currents and reworked by a current system flowing obliquely or normally to this main stream (Figures F6, F7). This current pattern filled the Inner Sea from west to east (Lüdmann et al., 2013). Starting with Drift Sequence (DS) 6, the opening of a southern gateway introduced northward flow of bottom waters in the Inner Sea, leading to deposition of giant elongated drifts at the eastern flank of the basin, filling it from east to west. Because the current swept away most of the material around the atolls, the system was not able to prograde and the steady subsidence was compensated by aggradation (Betzler et al., 2013a; Lüdmann et al., 2013).

DS1–DS9 are mostly conformable in the central part of the Inner Sea, but they display downlaps and onlaps at the basin margins. Two main types of bottom current–controlled deposits occur: (1) a prograding wedge to clinoform type near the passages between the atolls and (2) a mounded shape type located along the atoll flanks with a broad moat of 2.2–2.5 km in updip direction (Lüdmann et al., 2013). The latter is interpreted as a plastered drift body of a giant elongated drift, migrating along the basin flank under a weak current regime (Faugères et al., 1999). Narrower moats (500–800 m) at the western flank of the Inner Sea are interpreted as reflecting a high-velocity current focused in the west and a wider, slower current in the east. This partitioning is in line with monsoonal-triggered current reversals.

Two additional drowning steps affected the Maldives in the upper Miocene and lower Pliocene (Betzler et al., 2009, 2013a) (Figure F8). Flat-topped and atoll-shaped banks are interpreted to have drowned quickly, whereas mound-shaped banks are interpreted to have undergone sequential drowning under elevated nutrient fluxes (Betzler et al., 2009), similar to banks described by Zampetti et al. (2004) offshore Malaysia. The drowned banks are elongated parallel to the extension of the Kardiva Channel, which is characterized by throughflow of monsoon-driven surface currents and globally driven bottom currents (Lüdmann et al., 2013). This shape is interpreted as reflecting current control, similar to the recent atolls, which are elongated because of the action of waves and currents (Purdy and Bertram, 1993).

Partial drowning steps triggered by currents

Marine records suggest onset of monsoonal-triggered marine upwelling at ~8.5 Ma (Kroon et al., 1991). An increase in sediment flux into the Indian Ocean occurred around 11 Ma (Rea, 1992; Zheng et al., 2004), and a peak in the sedimentation rates of the Indus Fan occurred between 16 and 10 Ma (Clift et al., 2008). Onset and monsoon-intensification steps correlate with the Maldives partial drowning steps (Betzler et al., 2003a). It is therefore proposed that upwelling from monsoonal currents shaped the atolls in the past, controlling sediment production and reef growth. Thus, timing of the partial platform drowning and monsoon evolution is linked. Under monsoon conditions, upwelling injected nutrients into surface waters, affecting the carbonate banks (Betzler et al., 2009). Even short-term seasonal upwelling forces adaptation of the carbonate factory (Reijmer et al., 2012), controlling a biotic association with low growth potential more vulnerable to sea level change effects. This process caused the barrier reef demise, which was replaced by a string of current-shaped relict reefs, separated by passages accommodating the throughflow of currents (Betzler et al., 2009, Lüdmann et al., 2013).

Seismic studies/site survey data

Table **T1** provides characteristics of horizons tied into the available seismic data of the Maldives. The stratigraphic framework was established for the succession above the Oligocene/Miocene boundary, as the imaging quality of older strata is regarded to be too poor for interpretation. It is based on published horizons O/M, EM1, E/MM, MM3, MM5 (Belopolsky and Droxler, 2004a), and PB2 (Purdy and Bertram, 1993), which set a reliable stratigraphic framework throughout the Shell and Elf seismic grid and are tied into the newer high-resolution seismic data (Figure **F5**). In addition to the established horizons, the new high-resolution seismic lines allow us to trace a better approximation of the base of the middle Miocene (bMMio), as defined by Belopolsky and Droxler (2004a) at Well ARI-1, and the base of the early Pliocene (bEPlio), defined at Site 716 (Rio et al., 1990), throughout the seismic grid.

Supporting site survey data for Expedition 359 are archived at the **IODP Site Survey Data Bank**. Site survey data consist of multichannel reflection seismic lines and parasound lines acquired during R/V *Meteor* cruise M74/4 in December 2007 (Betzler et al., 2009, 2013a; Lüdmann et al., 2013) and the integration of the published low- to medium-resolution industrial reflection seismic Lines 1973/74 shot for Elf (Purdy and Bertram, 1993; Aubert and Droxler, 1996) and Lines 1989/90 for Shell (Belopolsky and Droxler, 2004), respectively. The Shell seismic data set covers the Inner Sea and the interatoll passages. The Elf seismic grid also transects most of the Maldivian atolls and offers good penetration depth across the atolls and their drowned parts. Stratigraphic interpretation of seismic data is made via correlation to published data of exploration Wells NMA-1 and ARI-1 and Site 716. This study is complemented by multibeam and parasound data, which were continuously recorded during the *Meteor* cruise.

The high-resolution seismic data set consists of approximately 1400 km of reflection seismic profiles. Seismic signals were generated by 2 clustered generator-injector (GI) guns, each with a volume of 45 in^3 for a 105 in^3 generated injector volume. A digital 144-channel streamer array with an active length of 600 m and an asymmetric group interval was used. The data were digitized with 7 SeaMUX 24-channel 24-bit digitizing modules, configured in 6 multiple arrays totaling 144 channels. The shotpoint distance during the entire cruise was 12.5 m. The dominant frequencies center around 100–120 Hz. Processing of reflection seismic data was done using the software package ProMAX 2-D (Halliburton-Landmark). The data are processed to zero phase, filtered in time and f-k domain, and corrected for dip moveout. In basinal areas, suppression of multiple reflections was achieved by predictive deconvolution of prestacked data. Amplitude losses were compensated by a power function. Interpretation and visualization was done using the software package Petrel (Schlumberger). Depending on depth, the vertical resolution of the newly acquired data is approximately 4–6 m compared to only 10–25 m of the Shell seismic data (Belopolsky and Droxler, 2004). The vertical resolution of the Elf seismic data is lower. Seismic interpretation was performed on time-migrated data in time domain. As the continuity of the reflections in part is weak, the instantaneous phase was also used for tracing.

An overview of the acquisition parameters and processing steps is as follows:

- Survey speed: average 5 nm;
- 144-channel digital streamer;
- Active length: 600 m;
- Group interval: asymmetric (average = 6.25);
- Shot interval: 12.5 (25 m p65 only);
- Sample rate: 1 ms;
- Offset source, first receiver: 55 m;

- Fold: 72 (p65 only) to 144;
- Common depth point (CDP) interval: 12.5 m;
- Source: 2 GI guns, total volume 300 in^3;
- Source frequency: 80–120 Hz;
- Software: Halliburton-Landmark ProMAX 2-D;
- Trace editing;
- Bandpass: Ormsby, frequency domain, 20-25-200-220;
- Minimum phase predictive deconvolution (multiple suppression);
- Designature (remove of source signature; transformation to zero-phase);
- Spherical divergence correction;
- Surface consistent amplitude recovery;
- Normal moveout (NMO) correction;
- Dip moveout (DMO) correction;
- Stack (mean);
- Fast explicit frequency domain (FD) time migration (12.5 m interval, max. freq. = 200 Hz);
- Automatic gain control (AGC) (1024 ms);
- SEG-Y export (ibm reel); and
- CDP locations: Projection UTM_WGS84_43N.

Subbottom profiles were recorded using the Parasound system on the *Meteor* in 2007. The system operates with 2 frequencies (18 and 22 kHz) emitted in a 4° cone from 2 hull-mounted transducers. The Parasound system uses the parametric effect caused by the interference of 2 frequencies in the water column. The effective signal of the Parasound is a 4 kHz wavelet, which results a seismic footprint with a diameter of 7% of the water depth. The seafloor penetration depth can reach up to about 200 m but varies strongly with the lithology, grain size, and gas load of the sediment.

Recorded data were stored in the Parasound native format ps3 and the raw-data format ASD for later processing. For onboard visualization, ps3 data were converted with the tool ps3segy (Hanno Keil, University of Bremen, Germany) into the standard seismic data format SEG-Y. Onboard data processing was performed with the software ReflexW (Sandmeier Software) and comprises AGC and amplitude normalization along the profile. Long profiles were subject to trace stacking in order to reduce the data volume. Processed data were stored in SEG-Y format for further visualization and interpretation in the software packages Kingdom Suite (IHS) and Petrel (Schlumberger).

Geological setting of the Kerala-Konkan Basin

Proposed Site KK-03B is positioned ~220 km offshore India at the edge of the Kerala-Konkan Basin (Figures **F1, F9**) that formed during the Mesozoic rifting of Gondwanaland (Kalaswad et al., 1993). Climate and the oceanographic setting of the site is similar to the Maldives and controlled by the seasonally reversing Indian monsoon system (Tomczak and Godfrey, 2003). A basement ridge, the Pratap Ridge, runs parallel to India's coast in the upper continental slope region, delineating a series of offshore basins under the shelf and upper slope (Naini and Talwani, 1982; Subrahmanyam et al., 1991). These basins contain 2–4 km of sediment (Rao, 2001; Campanile et al., 2008). Farther offshore, the Chagos-Laccadive Ridge parallels the southwestern margin of India south of ~15°N and continues across the Indian Ocean as the trace of the Réunion hotspot (Duncan, 1990). The drill site is located on line with the Chagos-Laccadive Ridge just north of it where it fades away as a bathymetric feature (Collet et al., 2008) (Figure **F10**). A basement high near the site comes to within 450 m of the seafloor. Isopach maps show slightly less than 1000 m of sediment in this region (Campanile et al., 2008) compared to more than 3 km north of the site in the Bombay Basin and south in the Kerala-Konkan Basin proper (Figure **F9**). Western India has a well-defined Cretaceous escarpment, the Western Ghats, that runs parallel to the coast at an average height of 1200 m. Monsoonal rains fall preferentially at the coast under this orographic influence (Xie et al., 2006). Surface waters at Site KK-03B are exposed to low-salinity summer monsoon conditions from direct rain, from fluvial discharge of Ghats rivers, as well as from the Bay of Bengal low-salinity sea-surface currents coming around the southern tip of India in winter (Jensen, 2001).

Drilling by the National Gas Hydrate Program of India at Site NGHP 01-1A located nearby yielded a continuous 300 m thick upper Eocene-recent sequence of hydrate- and turbidite-free, pelagic foraminifer-rich sediments with secondary siliciclastics (Collet et al., 2008) (Figures **F11, F12**). Seismic data show parallel stratification at the site without structural complications. The age model for Site NGHP 01-1A by Flores et al. (in press) shows that sedimentation was continuous for the last 35 My with bulk average sedimentation rates increasing significantly after ~9–8 Ma, with a gradual increase since ~18 Ma. Site KK-03B is expected to recover a similar but expanded section. These changes in sedimentation rate are accompanied by changes in (1) terrigenous vs. pelagic components; (2) clay mineral assemblage toward more illite dominated (Phillips et al., in press), indicative of physical weathering; and (3) possible increased inputs of C_4-type plant-derived organic carbon indicative of arid conditions (Johnson et al., in press).

Scientific objectives

The objectives for Expedition 359 relate to two challenges expressed in the IODP Initial Science Plan. The first addresses the variations in regional monsoon systems over multimillion-year timescales. The second addresses the question of how ice sheets and sea level respond to a warming climate, reducing the uncertainties in our understanding of the magnitude and rate of past sea level change. The specific objectives of Expedition 359 are as follows.

1. To decipher the record of Neogene environmental changes in the Maldives sediment archive.

The investigated environmental changes are primarily sea level and current evolution recorded in the prograding carbonate platform margins and drift sequences, respectively. Betzler et al. (2000) show that the major Cenozoic carbonate banks of the Bahama Bank (Atlantic Ocean; ODP Leg 166) and the Queensland Plateau (northeast Australia; ODP Leg 133) recorded sea level changes and synchronous oceanographic and atmospheric circulation events through compositional and architectural changes. Isern et al. (2004), Eberli et al. (2010), and John et al. (2011) argue for the combined effect of eustacy and variation in ocean currents determining the Miocene Marion Plateau stratigraphic record (ODP Leg 194). Previously, the Maldives platform evolution was ubiquitously related to sea level changes (Belopolsky and Droxler, 2004a, 2004b). This model has recently been challenged based on new seismic and hydroacoustic data sets (Figure **F4**) that show that the carbonate edifice contains major sediment drift bodies, indicating that currents (i.e., environmental changes) were a major driver of its evolution (Betzler et al., 2009, 2013a, 2013b; Lüdmann et al., 2013).

The global middle Miocene climatic optimum was followed by late middle Miocene cooling (Zachos et al., 2001), a reorganization of ocean circulation (Woodruff and Savin, 1989; Flower and Kennett, 1994), deepwater cooling (Lear et al., 2000), and substantial growth of the East Antarctic Ice Sheet (Lewis et al., 2007). Indonesian throughflow changes associated with the Neogene evolution of the Indonesian Gateway and closure of the Tethyan Seaway resulted in reduced atmospheric heat transport from the tropics to the high latitudes in the Indian and Pacific Ocean realms (Flower and Kennett, 1994). Enhanced uplift of the Himalayan region (Clift et al., 2008) concurs with the installation of the seasonally reversing Indian monsoon, resulting in coastal upwelling and increased terrigenous influx to the Indian Ocean (Kroon et al., 1991; Rea, 1992; Zheng et al., 2004). In addition, fluctuations in polar ice volume apparently controlled eustatic sea level variations (Miller et al., 1991, 2005, 2011).

Expedition 359 in the Maldives is designed to recover this mostly unread Indian Ocean archive of the evolving Cenozoic icehouse world from the thick carbonate edifice above Eocene volcanic basement. The Maldives, with its open ocean setting, is a key area for recording this global evolution. Proposed Sites MAL-01 through MAL-07 in the Inner Sea of the Maldives are arranged into two transects from platform to hemipelagic periplatform settings (Figure **F2**). Lithology and age data from the cores will record changes and turnovers of the neritic carbonate factories and link these changes to paleoenvironmental and paleoceanographic signals recorded in hemipelagic and pelagic series. Changes of the neritic carbonate factory will allow reconstruction of paleoenvironmental changes such as variations in the trophic structure of the water column or sea level changes. Horizons with subaerial exposures of platform carbonates will document times of sea level lowering. The strata in the distal parts of the transects will provide data for dating the changes observed in the platform, applying the usual combination of biostratigraphy and paleomagnetics.

2. To place the Maldives current system into the larger scale ocean current framework present during Neogene global cooling and monsoon evolution.

Mounded drift sequences are the sedimentary bodies deposited by ocean currents acting in the Maldives. Sequence boundaries and internal changes in the arrangement and geometry of reflection patterns attest for changes in current activity and strength through time. Cores from drill holes positioned in the drifts will add direct sedimentological evidence to the seismic-derived model of changing current patterns proposed in Lüdmann et al. (2013). Downhole logging and physical property data measured on the cores are crucial elements for linking seismic geometries with core data. In addition, higher frequency changes will be extracted through bulk sediment grain-size analysis, supported by analysis of grain-size variations of the sortable silt. The tight core coverage will result in an exact age model for these changes so that they can be compared and correlated to Indian Ocean–wide (Gourlan et al., 2008) and global changes in circulation. Because the current system is directly linked to the monsoon system, the drift sequences are expected to provide an extensive record into monsoon history from its onset in the middle Miocene to the present.

3. To obtain a continuous carbon isotopic record to calibrate a platform and platform margin record with the pelagic record.

A major transfer of carbon from the organic to inorganic reservoirs characterizes the Neogene. This transfer is manifested in the large change in the $\delta^{13}C$ of oceanic carbonates documented in various records (Shackleton, 1985; Zachos et al., 2001), which has been modeled by various workers (Kump and Arthur, 1999). Carbon isotopic records from carbonate sediments and their associated organic material offer perhaps the best opportunity for the reconstruction of the global carbon cycle (Hayes et al., 1999; Kump and Arthur, 1999). Although open oceanic pelagic records offer the best records for reconstruction of the global carbon cycle (Shackleton, 1985), for the ancient history of Earth we are forced to rely on records of platform-derived sediments (Veizer et al., 1999). It is therefore particularly important to calibrate $\delta^{13}C$ in periplatform settings against oceanic records over the same time period. It has been shown that global correlation of $\delta^{13}C$ can exist between different carbonate margins that are not correlated to a global carbon cycle (Swart, 2008). The proposed drilling offers the opportunity to obtain a complete record through the Miocene that can be correlated to adjacent ODP sites (i.e., Leg 115 sites) and notable carbon isotopic events (i.e., Monterey carbon excursion) that occurred during the Neogene. The Indian Ocean experienced a complicated history of changes in mass carbonate accumulation related to production during the Miocene, as well as changes in the carbonate compensation depth (Backman, Duncan, et al., 1988; Peterson and Backman, 1990); therefore, such a comparison will enable precise correlation between records such as those obtained from ODP Site 709 (Baker et al., 1990) and Expedition 359 sites. The results will enable an assessment of the competing influences of source and diagenesis relative to oceanic changes in the control of the carbon isotopic composition or the organic and carbonate components.

4. To reconstruct the Cenozoic paleoclimate of the Indian Peninsula.

The onset and intensification phases and the complete Cenozoic evolution of the Indian monsoon remain controversial. There is a lack of consensus regarding the onset or intensification of the Indian monsoon (e.g., Allen and Armstrong, 2012). Some proxy records suggest that the initial intensification occurred at ~7 to 8 Ma (e.g., Kroon et al., 1991; Prell et al., 1992), whereas others suggest a considerably earlier onset, as early as ~22 Ma (Clift et al., 2008; Guo et al., 2002) or the Eocene (Licht et al., 2014). Alternatively, events at ~8 Ma were linked to global cooling (Gupta et al., 2004) or coupled to productivity changes (Filippelli, 1997). Similarly, little consensus exists on the ultimate forcing of monsoon winds and precipitation at orbital timescales (e.g., An et al., 2011; Clemens et al., 2010; Ruddiman, 2006). Detailed long-term monsoon records over the Indian peninsula, south of the Himalayas, are essentially nonexistent. Proposed Site KK-03B will provide the opportunity to reconstruct colocated oceanic and terrestrial records at a location free of any direct influence from the glaciated Himalaya and Tibet. This will allow deciphering the effects of tectonics and premonsoonal/monsoonal climate change on erosion, weathering, and runoff. The final goal is to establish the sensitivity and timing of changes in monsoon circulation relative to external insolation forcing and internal boundary conditions over the Cenozoic. Another important objective for Site KK-03B is to determine the expression of the Paleogene/Eocene Thermal Maximum in a foraminifer-rich pelagic setting in the northern Indian Ocean. Fulfilling this task will depend on the drilled depth and yet-unknown Eocene sedimentation rates.

Relationship with previous drilling

Stratigraphic data for industrial Wells NMA-1 and ARI-1 and Site 716 are presented in Purdy and Bertram (1993), Aubert and Droxler (1996), Belopolsky and Droxler (2004a), and Rio et al. (1990). These sources provide the chronostratigraphic framework for the seismic interpretation. Carbonate lithofacies, paleobathymetric evaluations, and biostratigraphic age determinations based on cuttings and sidewall core analysis for Shell exploration Well ARI-1 were first published by Aubert and Droxler (1996). A vertical seismic profile is used for time-depth conversion and to tie well data to seismic data (Figure **F3**). For Site 716, which is covered by two high-resolution seismic lines (Figures **F3, F4**), a simple time-depth estimation is made based on existing whole-core *P*-wave velocity measurements.

Site 716, drilled in the Inner Sea, recovers the topmost DS4 to DS9. The 264 m thick periplatform ooze bears a mixed record of sea level and bottom-current velocity changes (Lüdmann et al., 2013; Betzler et al., 2013b); grain-size variations for the last 7 My correlate with DS boundaries. Further, the amount of the fine fraction varies, providing insights into past bottom-current speed fluctuations.

For the last 2 My, coarser deposits formed at times (~1.5–0.34 Ma) of an intensified monsoon regime (Betzler et al., 2013b), as presented in Zhisheng et al. (2011). During the early mid-Pleistocene transition, the first large Pleistocene sea level fall triggered deposition of a grain-flow interval in the Inner Sea; subsequently, a strong bottom current led to winnowing of fines at the seafloor. With weakening of the monsoon system around marine isotope stage (MIS) 10, Site 716 grain-size variations become positively correlated with oxygen isotope data and aragonite contents, resembling the sawtooth pattern of Late Pleistocene glacial–interglacial cycles. This reflects highstand shedding from the shallow banks (Paul et al., 2012; Betzler et al., 2013b).

For deposits older than 2–3 Ma, the published record of monsoon strength is patchy and in part contradictory (Kroon et al., 1991; Rea et al., 1992; Clift et al., 2008). Therefore, only a limited and preliminary comparison of Site 716 grain-size data with monsoon proxies is feasible (Figure **F7**). This comparison indicates that bottom current strength was possibly decoupled from the monsoon system and that the Maldives drift sequences may record variations in the intermediate water flow (Lüdmann et al., 2013). Data indicate that current speed rose between 8 and 5 Ma and was high from 5 to 3 Ma.

In summary, sedimentological analysis of Site 716 shows that periplatform ooze not only records highstand shedding of the atolls but also fluctuations in the bottom current regime, further implying that periplatform ooze, which accumulated in sediment drifts, contains a potential multivariable record of fluctuations of past changes.

The Maldives, located close to India and directly influenced by the monsoon climate, are expected to provide extensive insight into the monsoon history starting from its onset in the middle Miocene to the present. This expedition forms an important complement to work proposed for monsoon-dedicated IODP expeditions. In contrast to these sites at gravity-controlled siliciclastic continental margin settings, the drift deposits of the Maldives represent a continuous time record not disrupted by intercalated mass flow events or major hiatuses, as shown by Site 716. A combined look at independent settings may allow us, for the first time, to receive a complete record of past monsoon variability and contemporaneously help to obtain a better understanding of global climate changes.

Operations plan/drilling strategy

Expedition 359 aims to achieve an ambitious coring program that prioritizes 7 primary sites and 1 alternate site in 380–2400 m of water depth (Table **T2**). Six of the sites are in the Maldives archipelago and one is west of the Indian peninsula in the Arabian Sea (Figure **F1**). The final operations plan and number of sites to be cored (Table **T3**) is contingent upon the *JOIDES Resolution* operations schedule, operational risks (see **Risks and contingency**), and the outcome of requests for territorial permission to occupy these sites. Of particular relevance is the planned ~14 day transit from Darwin, Australia, prior to beginning coring operations in the Maldives. Should ship speed be less than the estimated average of 10.5 kt, the drilling schedule could be significantly impacted. The current planned operations schedule also includes two half-day moorings for required ship clearance and immigration formalities, one at the arrival to and one at the exit from the Maldives.

The planned sequence of drill sites, coring/downhole measurements, and time estimates is provided in Tables **T3** and **T4.** For operational efficiency, the sites will be occupied in the following sequence: MAL-07A, MAL-05A, MAL-03A, MAL-02A, MAL-01A, MAL-04B, and KK-03B. The coring strategy will consist of triple advanced piston corer (APC) coring using nonmagnetic core barrels to ~200 meters below seafloor (mbsf) or to APC refusal at Sites MAL-07A, MAL-03A, and KK-03B. Coring using the extended core barrel (XCB) system will be used to advance the holes to total depths at Sites MAL-07A (642 mbsf), MAL-03A (435 mbsf), MAL-02A (325 mbsf), MAL-04B (554 mbsf), and KK-03B (450 mbsf). Coring with the rotary core barrel (RCB) system will be used to advance to total depth at Sites MAL-05A (420 mbsf), MAL-01A (1060 mbsf), and MAL-02A (560 mbsf). As described below and pending further discussions, at this point only cores from Hole A at each site will be oriented.

For planning purposes, APC refusal depth is estimated at 200 mbsf, although we anticipate that this may be exceeded at some of the more mud rich sites with target depths greater than 200 mbsf. On the other hand, we estimate that APC refusal may be reached at a shallower depth at Sites MAL-05A, MAL-01A, and MAL-04B because of the presence of lithified carbonate sediments (e.g., limestones). APC refusal is conventionally defined in two ways: (1) a complete stroke (as determined from the standpipe pressure after the shot) is not achieved because the formation is too hard or (2) excess force (>100,000 lb) is required to pull the core barrel out of the formation because the sediment is too cohesive or "sticky." In cases where a significant stroke can be achieved but excessive force cannot retrieve the barrel, the core barrel can be "drilled over" (i.e., after the inner core barrel is successfully shot into the formation, the bit is advanced to some depth to free the APC barrel). When APC refusal occurs in a hole before the target depth is reached, the half-length APC system may be used to advance the hole before switching to the XCB technique (see Tables **T3** and **T4** for operations details per site). All target depths in the current operations plan for sites within the Maldives archipelago have been approved by the IODP Environmental

Protection and Safety Panel and the Texas A&M University Safety Panel, but a request to extend the penetration depth at Site MAL-02A to 1060 mbsf will be submitted after publication of this *Scientific Prospectus*. EPSP approval also is pending for the drill sites in the Kerala-Konkan Basin (proposed Sites KK-03A and KK-03B) and will be requested at the same time as the depth penetration extension. Triple APC holes will allow us to build a composite stratigraphic section at each site for the upper ~200 mbsf and deeper at Site KK-03B, where double XCB will be used below APC refusal.

According to the current operations plan, Expedition 359 will core ~5400 m of sediment and potentially recover ~4100 m of core. The estimate of the amount of core recovered is based on 100% recovery with the APC system, 65% recovery with the XCB system, and 50% with the RCB system. Considering the significant transit time at the beginning of the expedition (~2 weeks), this coring schedule within the remaining 6 weeks of the expedition is indeed ambitious and will require tight operational planning and flexibility.

Logging/downhole measurements strategy

Because of the high priority of seismic-core integration, all sites except Site KK-03B will be wireline logged. The downhole measurement plan aims to provide a broad set of parameters that can be used for the characterization of in situ formation properties (lithologies, structures, and petrophysics) and orbital- and millennial-scale cyclicities. The plan includes the use of different tool strings (details at **iodp.tamu.edu/tools/logging/index.html**).

The triple combination (triple combo) tool string logs formation resistivity, density, porosity, natural gamma radiation (NGR), and borehole diameter. A diameter log is provided by the caliper on the density tool to allow assessment of hole conditions (e.g., washouts of sandy beds), log quality, and the potential for success of the following runs. NGR data gathered by the triple combo may prove useful for correlation with ship-based NGR measurements.

The paleocombo tool string is a modified triple combo in which a newly built magnetic susceptibility sonde (MSS) replaces the porosity sonde. Results can be correlated with magnetic susceptibility measurements from whole-round cores. As with the triple combo, NGR data gathered by the paleocombo may prove useful for correlation with the ship-based NGR instrument.

The Formation MicroScanner (FMS)-sonic tool string provides an oriented 360° high-resolution resistivity image of the borehole wall and logs of formation acoustic velocity and borehole diameter. Sonic logs can be combined with triple combo density logs to generate synthetic seismograms and provide high-resolution seismic-well integration. A NGR tool will also be run on the FMS-sonic tool string to depth-match the different logging runs and perhaps correlate to the ship-based NGR instrument.

The Versatile Seismic Imager (VSI) tool string, which is used to acquire a zero-offset vertical seismic profile (VSP) for high-resolution integration of borehole stratigraphy and seismic profile, may be used at some sites, in particular Sites MAL-01A, MAL-04B, MAL-07A, pending time availability and permission from the National Science Foundation to conduct the operation in compliance with IODP marine mammal protection policy. A check shot survey planned with ~50 m spacing of stations over the entire open hole interval will give depth to seismic traveltime conversions. The seismic source for the check shots will be a GI air gun, and its deployment is also subject to the IODP marine mammal policy. The check shot survey will be postponed or canceled if policy conditions are not met.

Downhole measurements will be the only data available where core recovery is incomplete. Moreover, the data will provide common measurements for core-log integration (density, NGR, and magnetic susceptibility) and establish the link between borehole and core features and reflectors on seismic profiles by synthetic seismograms and VSPs.

Risks and contingency

The principal operational risks identified for this expedition include

- Obtaining approval from the Republic of the Maldives and India to conduct drilling and coring operations in their territorial waters.
- Obtaining permission from the National Science Foundation to conduct VSI operation and successfully implementing the seismic experiments.
- Shallow-water coring.
- Weather. Although the expedition has been scheduled take place in fall, severe weather may still occur and could adversely impact operations.
- Alternating lithologies, which may lead to hole instability. Successful coring and wireline logging depends upon good hole conditions. Deep XCB coring depths

could be problematic (may require roundtrip of the drill string and coring with the RCB system).

- An extremely ambitious operations plan for the time available. Good time management will be extremely important to mitigate this risk.
- No special risks beyond those outlined above for Site KK-03B based on previous drilling by India's National Gas Hydrates Project (NGHP).

All of these factors may affect coring and drilling operations.

Sampling and data sharing strategy

Shipboard and shore-based researchers should refer to the IODP Sample, Data, and Obligations Policy and Implementation Guidelines (**www.iodp.org/program-documents**). This document outlines the policy for distributing IODP samples and data to research scientists, curators, and educators. The document also defines the obligations that sample and data recipients incur. The Sample Allocation Committee (SAC; composed of the Co-Chief Scientists, Staff Scientist, and IODP Curator on shore and a curatorial representative on board ship) will work with the entire scientific party to formulate a formal expedition-specific sampling plan for shipboard and postcruise sampling.

Every member of the science party is obligated to carry out scientific research for the expedition and publish the results. For this purpose, shipboard scientists are expected to submit research plans and sample requests 3 months before the beginning of the expedition (**web.iodp.tamu.edu/sdrm**). Based on sample requests (shore based and shipboard) submitted by this deadline, the SAC will prepare a tentative sampling plan that will be revised on the ship as dictated by recovery and cruise objectives. The sampling plan will be subject to modification depending on the actual material recovered and collaborations that may evolve between scientists during the expedition. Given the range of specific objectives for Expedition 359, great care will be taken to maximize shared sampling to promote integration of data sets and enhance scientific collaboration among members of the scientific party. This planning process is necessary to coordinate the research to be conducted and to ensure that the scientific objectives are achieved. Modifications to sample requests and access to samples and data during the expedition and the 1 y postexpedition moratorium period will require approval by the SAC.

The minimum permanent archive will be the standard archive half of each core. All sample frequencies and sizes must be justified on a scientific basis and will depend on core recovery, the full spectrum of other requests, and the cruise objectives. Some redundancy of measurement is unavoidable, but minimizing the duplication of measurements among the shipboard party and identified shore-based collaborators will be a factor in evaluating sample requests.

If some critical intervals are recovered, there may be considerable demand for samples from a limited amount of cored material. These intervals may require special handling, a higher sampling density, reduced sample size, or continuous core sampling by a single investigator. A sampling plan coordinated by the SAC may be required before critical intervals are sampled. Success will require collaboration, integration of complementary data sets, and consistent methods of analysis. Substantial collaboration and cooperation between members of the science party are highly encouraged.

Shipboard sampling will be restricted to acquiring ephemeral data types and to limited low-resolution sampling (e.g., for stratigraphic purposes [biostratigraphy and magnetostratigraphy], physical properties, and geochemical and microbiological analyses). Shipboard biostratigraphic and paleomagnetostratigraphic sampling will also be restricted to rapidly produce age models that are critical to the overall objectives of the expedition and to planning for higher resolution postcruise sampling. The shipboard sampling strategy for analyses conducted during the expedition must be approved by the Co-Chief Scientists, Staff Scientist, and curatorial representative on board ship.

Sampling for the majority of individual scientist's personal research will be postponed until a shore-based sampling party implemented between 3 and 5 months after the expedition at the Kochi Core Center (KCC) at Kochi University in Kochi, Japan. The KCC repository houses cores from the Pacific Ocean (west of the western boundary of the Pacific plate), Indian Ocean (north of 60°), Kerguelen Plateau, and Bering Sea. Limited low-resolution sampling of selected sites or cored sections that may not require multihole stratigraphic correlation may be conducted during the expedition given time availability and SAC approval.

All collected data and samples will be protected by a 1 y postcruise moratorium, during which time data and samples will be available only to the Expedition 359 science party and approved shore-based participants. This moratorium will extend 1 y following the completion of the postcruise sampling party (not 1 y from the end of the time at sea). We anticipate that specific shipboard and shore-based scientific party members may require specific sampling methods. For example, Rhizon sampling may be requested for high-resolution or trace metal clean pore water sampling, and microbiological sampling often requires rapid sample processing.

References

Allen, M.B., and Armstrong, H.A., 2012. Reconciling the Intertropical Convergence Zone, Himalayan/Tibetan tectonics, and the onset of the Asian monsoon system. *Journal of Asian Earth Sciences*, 44:36–47. **http://dx.doi.org/10.1016/j.jseaes.2011.04.018**

Aubert, O., and Droxler, A.W., 1992. General Cenozoic evolution of the Maldives carbonate system (equatorial Indian Ocean). *Bulletin Des Centres de Recherches Exploration-Production Elf-Aquitaine,* 16(1):113–136.

Aubert, O., and Droxler, A.W., 1996. Seismic stratigraphy and depositional signatures of the Maldive carbonate system (Indian Ocean). *Marine and Petroleum Geology*, 13(5):503–536. **http://dx.doi.org/10.1016/0264-8172(96)00008-6**

Backman, J., Duncan, R.A., et al., 1988. *Proceedings of the Ocean Drilling Program, Initial Reports,* 115: College Station, TX (Ocean Drilling Program). **http://dx.doi.org/10.2973/odp.proc.ir.115.1988**

Baker, P.A., Malone, M.J., Burns, S.J., and Swart, P.K., 1990. Minor element and stable isotopic composition of the carbonate fine fraction: Site 709, Indian Ocean. *In* Duncan, R.A., Backman, J., Peterson, L.C., et al., *Proceedings of the Ocean Drilling Program, Scientific Results,* 115: College Station, TX (Ocean Drilling Program), 661–675. **http://dx.doi.org/10.2973/odp.proc.sr.115.178.1990**

Belopolsky, A.V., and Droxler, A.W., 2004a. Seismic expressions and interpretation of carbonate sequences: the Maldives platform, equatorial Indian Ocean. *AAPG Studies in Geology,* 49. **http://archives.datapages.com/data/specpubs/study49/images/st49.pdf**

Belopolsky, A.V. and Droxler, A.W., 2004b. Seismic expressions of prograding carbonate bank margins: middle Miocene, Maldives, Indian Ocean. *In* Eberli, G.P., Masaferro, J.L., and Sarg, J.F. (Eds.), *Seismic Imaging of Carbonate Reservoirs and Systems*. AAPG Memoir, 81:267–290. **http://archives.datapages.com/data/specpubs/memoir81/CHAPTER12/CHAPTER12.HTM**

Betzler, C., Fürstenau, J., Lüdmann, T., Hübscher, C., Lindhorst, S., Paul, A., Reijmer, J.J.G., and Droxler, A.W., 2013a. Sea-level and ocean-current control on carbonate-platform growth, Maldives, Indian Ocean. *Basin Research*, 25(2):172–196. **http://dx.doi.org/10.1111/j.1365-2117.2012.00554.x**

Betzler, C., Hübscher, C., Lindhorst, S., Reijmer, J.J.G., Römer, M., Droxler, A.W., Fürstenau, J., and Lüdmann, T., 2009. Monsoon-induced partial carbonate platform drowning (Maldives, Indian Ocean). *Geology*, 37(10): 867–870. **http://dx.doi.org/10.1130/G25702A.1**

Betzler, C., Kroon, D., and Reijmer, J.J.G., 2000. Synchroneity of major late Neogene sea level fluctuations and paleoceanographically controlled changes as recorded by two carbonate platforms. *Paleoceanography,* 15(6):722–730. **http://dx.doi.org/10.1029/1999PA000481**

Betzler, C., Lüdmann, T., Hübscher, C., and Fürstenau, J., 2013b. Current and sea-level signals in periplatform ooze (Neogene, Maldives, Indian Ocean). *Sedimentary Geology*, 290:126–137. **http://dx.doi.org/10.1016/j.sedgeo.2013.03.011**

Camoin, G.F., Seard, C., Deschamps, P., Webster, J.M., Abbey, E., Braga, J.C., Iryu, Y., Durand, N., Bard, E., Hamelin, B., Yokoyama, Y., Thomas, A.L., Henderson, G.M., and Dussouillez, P., 2012. Reef response to sea-level and environmental changes during the last deglaciation: Integrated Ocean Drilling Program Expedition 310, Tahiti Sea Level. *Geology*, 40(7): 643–646. **http://dx.doi.org/10.1130/G32057.1**

Campanile, D., Nambiar, C.G., Bishop, P., Widdowson, M., and Brown, R., 2008. Sedimentation record in the Konkan-Kerala Basin: implications for the evolution of the Western Ghats and the Western Indian passive margin. *Basin Research*, 20(1):3–22. **http://dx.doi.org/10.1111/j.1365-2117.2007.00341.x**

Ciarapica, G., and Passeri, L., 1993. An overview of the Maldivian coral reefs in Felidu and North Malé Atoll (Indian Ocean): platform drowning by ecological crises. *Facies*, 28(1):33–65. **http://dx.doi.org/10.1007/BF02539727**

Clemens, S.C., Prell, W.L., and Sun, Y., 2010. Orbital-scale timing and mechanisms driving Late Pleistocene Indo-Asian summer monsoons: reinterpreting cave speleothem $\delta^{18}O$. *Paleoceanography,* 25(4):PA4207. **http://dx.doi.org/10.1029/2010PA001926**

Clift, P.D., Hodges, K.V., Heslop, D., Hannigan, R., Long, H.V., and Calves, G., 2008. Correlation of Himalayan exhumation rates and Asian monsoon intensity. *Nature Geoscience,* 1(12):875–880. **http://dx.doi.org/10.1038/ngeo351**

Collett, T.S., Riedel, M., Cochran, J.R., Boswell, R., Presley, J., Kumar, P., Sathe, A.V., Sethi, A., Lall, M., Sibal, V., and the NGHP Expedition 01 Scientific Party, 2008. *Indian National Gas Hydrate Program Expedition 01, Initial Reports:* Noida, India (Directorate General of Hydrocarbons, Ministry of Petroleum and Natural Gas).

Droxler, A.W., Haddad, G.A., Mucciarone, D.A., and Cullen, J.L., 1990. Pliocene–Pleistocene aragonite cyclic variations in Holes 714A and 716B (the Maldives) compared with Hole 633A (the Bahamas): records of climate-induced $CaCO_3$ preservation at intermediate water depths. *In* Duncan, R.A., Backman, J., Peterson, L.C., et al., *Proceedings of the Ocean Drilling Program, Scientific Results,* 115: College Station, TX (Ocean Drilling Program), 539–577. **http://dx.doi.org/10.2973/odp.proc.sr.115.179.1990**

Duncan, R.A., 1990. The volcanic record of the Réunion hotspot. *In* Duncan, R.A., Backman, J., Peterson, L.C., et al., *Proceedings of the Ocean Drilling Program, Scientific Results,* 115: College Station, TX (Ocean Drilling Program), 3–10. **http://dx.doi.org/10.2973/odp.proc.sr.115.206.1990**

Eberli, G.P., Anselmetti, F.S., Isern, A.R., and Delius, H., 2010. Timing of changes in sea-level and currents along Miocene platforms on the Marion Plateau, Australia. *In* Morgan, W.A., George, A.D., Harris, P.M., Kupecz, J.A., and Sarg, J.F. (Eds.), *Cenozoic Carbonate Systems of Australasia*. Special Publication—SEPM (Society for Sedimentary Geology), 95:219–242.

Eberli, G.P., Anselmetti, F.S., Kroon, D., Sato, T., and Wright, J.D., 2002. The chronostratigraphic significance of seismic reflections along the Bahamas Transect. *Marine Geology,* 185(1–2):1–17. **http://dx.doi.org/10.1016/S0025-3227(01)00287-0**

Erlich, R.N., Longo, A.P., Jr., and Hyare, S., 1993. Response of carbonate platform margins to drowning: evidence of environmental collapse. *AAPG Memoir*, 57:241–266. **http://archives.datapages.com/data/specpubs/seismic2/data/a168/a168/0001/0200/0241.htm**

Faugères, J.-C., Stow, D.A.V., Imbert, P., and Viana, A., 1999. Seismic features diagnostic of contourite drifts. *Marine Geology,* 162(1):1–38. **http://dx.doi.org/10.1016/S0025-3227(99)00068-7**

Filippelli, G.M., 1997. Intensification of the Asian monsoon and a chemical weathering event in the late Miocene–early Pliocene: implications for late Neogene climate change. *Geology,* 25(1):27–30. **http://dx.doi.org/10.1130/0091-7613(1997)025<0027:IOTAMA>2.3.CO;2**

Flores, J.A., Johnson, J.E., Mejía-Molina, A.E., Álverez, M.C., Sierro, F.J., Singh, S.D., Mahanti, S., and Giosan, L., in press. Sedimentation rates from calcareous nannofossil and planktonic foraminifera biostratigraphy in the Andaman Sea, northern Bay of Bengal, and eastern Arabian Sea. *Marine and Petroleum Geology*. **http://dx.doi.org/10.1016/j.marpetgeo.2014.08.011**

Flower, B.P., and Kennett, J.P., 1994. The middle Miocene climatic transition: East Antarctic ice sheet development, deep ocean circulation and global carbon cycling. *Palaeogeography, Palaeoclimatology, Palaeoecology,* 108(3–4):537–555. **http://dx.doi.org/10.1016/0031-0182(94)90251-8**

Fürstenau, J., Lindhorst, S., Betzler, C., and Hübscher, C., 2010. Submerged reef terraces of the Maldives (Indian Ocean). *Geo-Marine Letters*, 30(5):511–515. **http://dx.doi.org/10.1007/s00367-009-0174-2**

Gischler, E., 2006. Sedimentation on Rasdhoo and Ari atolls, Maldives, Indian Ocean. *Facies*, 52(3):341–360. **http://dx.doi.org/10.1007/s10347-005-0031-3**

Gischler, E., Hudson, J.H., and Pisera, A., 2008. Late Quaternary reef growth and sea level in the Maldives (Indian Ocean). *Marine Geology*, 250(1–2):104–113. **http://dx.doi.org/10.1016/j.margeo.2008.01.004**

Gourlan, A.T., Meynadier, L., and Allègre, C.J., 2008. Tectonically driven changes in the Indian Ocean circulation over the last 25 Ma: neodymium isotope evidence. *Earth and Planetary Science Letters,* 267(1–2):353–364. **http://dx.doi.org/10.1016/j.epsl.2007.11.054**

Guo, Z.T., Ruddiman, W.F., Hao, Q.Z., Wu, H.B., Qiao, Y.S., Zhu, R.X., Peng, S.Z., Wei, J.J., Yuan, B.Y., and Liu, T.S., 2002. Onset of Asian desertification by 22 Myr ago inferrred from loess deposits in China. *Nature,* 416(6877):159–163. **http://dx.doi.org/10.1038/416159a**

Gupta, A.K., Singh, R.K., Joseph, S., and Thomas, E., 2004. Indian Ocean high-productivity event (10–8 Ma): linked to global cooling or to the initiation of the Indian monsoons? *Geology,* 32(9):753–756. **http://dx.doi.org/10.1130/G20662.1**

Halfar, J., and Mutti, M., 2005. Global dominance of coralline red-algal facies: a response to Miocene oceanographic events. *Geology*, 33(6):481–484. **http://dx.doi.org/10.1130/G21462.1**

Hayes, J.M., Strauss, H., and Kaufman, A.J., 1999. The abundance of ^{13}C in marine organic matter and isotopic fractionation in the global biogeochemical cycle of carbon during the past 800 Ma. *Chemical Geology*, 161(1–3):103–125. **http://dx.doi.org/10.1016/S0009-2541(99)00083-2**

Isern, A.R., Anselmetti, F.S., and Blum, P., 2004. A Neogene carbonate platform, slope, and shelf edifice shaped by sea level and ocean currents, Marion Plateau (northeast Australia). *In* Eberli, G.P., Masaferro, J.L., and Sarg, J.F. (Eds.), *Seismic Imaging of Carbonate Reservoirs and Systems*. AAPG Memoir, 81:291–307. **http://archives.datapages.com/data/specpubs/memoir81/CHAPTER13/CHAPTER13.HTM**

Jensen, T.G., 2003. Cross-equatorial pathways of salt and tracers from the northern Indian Ocean: modeling results. *Deep Sea Research, Part II,* 50(12–13):2111–2127. **http://dx.doi.org/10.1016/S0967-0645(03)00048-1**

John, C.M., Karner, G.D., Browning, E., Leckie, R.M., Mateo, Z., Carson, B., and Lowery, C., 2011. Timing and magnitude of Miocene eustasy derived from the mixed siliciclastic-carbonate stratigraphic record of the northeastern Australian margin. *Earth and Planetary Science Letters,* 304(3–4):455–467. **http://dx.doi.org/10.1016/j.epsl.2011.02.013**

Johnson, J.E., Phillips, S.C., Torres, M.E., Piñero, E., Rose, K.K., and Giosan, L., in press. Influence of total organic carbon deposition on the inventory of gas hydrate in the Indian continental margins. *Marine and Petroleum Geology.* **http://dx.doi.org/10.1016/j.marpetgeo.2014.08.021**

Kalaswad, S., Roden, M.K., Miller, D.S., and Morisawa, M., 1993. Evolution of the continental margin of Western India: new evidence from apatite fission-track dating. *Journal of Geology,* 101(5):667–673. **http://www.jstor.org/stable/30080161**

Kroon, D., Steens, T., and Troelstra, S.R., 1991. Onset of monsoonal related upwelling in the western Arabian Sea as revealed by planktonic foraminifers. *In* Prell, W.L., Niitsuma, N., et al., *Proceedings of the Ocean Drilling Program, Scientific Results,* 117: College Station, TX (Ocean Drilling Program), 257–263. **http://dx.doi.org/10.2973/odp.proc.sr.117.126.1991**

Kump, L.R., and Arthur, M.A., 1999. Interpreting carbon-isotope excursions: carbonates and organic matter. *Chemical Geology,* 161(1–3):181–198. **http://dx.doi.org/10.1016/S0009-2541(99)00086-8**

Lear, C.H., Elderfield, H., and Wilson, P.A., 2000. Cenozoic deep-sea temperatures and global ice volumes from Mg/Ca in benthic foraminiferal calcite. *Science,* 287(5451):269–272. **http://dx.doi.org/10.1126/science.287.5451.269**

Lewis, A.R., Marchant, D.R., Ashworth, A.C., Hemming, S.R., and Machlus, M.L., 2007. Major middle Miocene global climate change: evidence from East Antarctica and the Transantarctic Mountains. *Geological Society of America Bulletin,* 119(11):1449–1461. **http://dx.doi.org/10.1130/0016-7606(2007)119[1449:MMMGCC]2.0.CO;2**

Licht, A., van Cappelle, M., Abels, H.A., Ladant, J.-B., Trabucho-Alexandre, J., France-Lanord, C., Donnadieu, Y., Vandenberghe, J., Rigaudier, T., Lécuyer, C., Terry, D., Jr., Adriaens, R., Boura, A., Guo, Z., Soe, A.N., Quade, J., Dupont-Nivet, G., and Jaeger, J.-J., 2014. Asian monsoons in a late Eocene greenhouse world. *Nature*, 513(7519):501–506. **http://dx.doi.org/10.1038/nature13704**

Lüdmann, T., Kalvelage, C., Betzler, C., Fürstenau, J., and Hübscher, C., 2013. The Maldives, a giant isolated carbonate platform dominated by bottom currents. *Marine and Petroleum Geology*, 43:326–340. **http://dx.doi.org/10.1016/j.marpetgeo.2013.01.004**

Miller, K.G., Kominz, M.A., Browning, J.V., Wright, J.D., Mountain, G.S., Katz, M.E., Sugarman, P.J., Cramer, B.S., Christie-Blick, N., and Pekar, S.F., 2005. The Phanerozoic record of global sea-level change. *Science,* 310(5752):1293–1298. **http://dx.doi.org/10.1126/science.1116412**

Miller, K.G., Mountain, G.S., Wright, J.D., and Browning, J.V., 2011. A 180-million-year record of sea level and ice volume variations from continental margin and deep-sea isotopic records. *Oceanography,* 24(2):40–53. **http://dx.doi.org/10.5670/oceanog.2011.26**

Miller, K.G., Wright, J.D., and Fairbanks, R.G., 1991. Unlocking the ice house: Oligocene–Miocene oxygen isotopes, eustasy, and margin erosion. *Journal of Geophysical Research: Solid Earth,* 96(B4):6829–6848. **http://dx.doi.org/10.1029/90JB02015**

Naini, B.R., and Talwani, M., 1982. Structural framework and the evolutionary history of the continental margin of Western India. *In* Watkins, J.S., and Drake, C.L. (Eds.), *Studies in Continental Margin Geology.* AAPG Memoir, 167–191.

Paul, A., Reijmer, J.J.G., Fürstenau, J., Kinkel, H., and Betzler, C., 2012. Relationship between Late Pleistocene sea-level variations, carbonate platform morphology and aragonite production (Maldives, Indian Ocean). *Sedimentology*, 59(5):1540–1658. **http://dx.doi.org/10.1111/j.1365-3091.2011.01319.x**

Peterson, L.C., and Backman, J., 1990. Late Cenozoic carbonate accumulation and the history of the carbonate compensation depth in the western equatorial Indian Ocean. *In* Duncan, R.A., Backman, J., Peterson, L.C., et al., *Proceedings of the Ocean Drilling Program, Scientific Results,* 115: College Station, TX (Ocean Drilling Program), 467–507. **http://dx.doi.org/10.2973/odp.proc.sr.115.163.1990**

Phillips, S.C., Johnson, J.E., Underwood, M.B., Guo, J., Giosan, L., and Rose, K., in press. Long-timescale variation in bulk and clay mineral composition of Indian continental margin sediments in the Bay of Bengal, Arabian Sea, and Andaman Sea. *Marine and Petroleum Geology.* **http://dx.doi.org/10.1016/j.marpetgeo.2014.06.018**

Prell, W.L., Murray, D.W., Clemens, S.C., and Anderson, D.M., 1992. Evolution and variability of the Indian Ocean summer monsoon: evidence from the western Arabian Sea drilling program. *In* Duncan, R.A., Rea, D.K., Kidd, R.B., von Rad, U., and Weissel, J.K. (Eds.), *Synthesis of Results from Scientific Drilling in the Indian Ocean.* Geophysical Monograph, 70:447–469. **http://dx.doi.org/10.1029/GM070p0447**

Preu, C., and Engelbrecht, C., 1991. Patterns and processes shaping the present morphodynamics of coral reef islands—case study from the North-Male atoll, Maldives (Indian Ocean). *In* Brückner, H., and Radtke, U. (Eds.), *From the North Sea to the Indian Ocean*: Stuttgart, Germany (Franz Steiner), 209–220.

Purdy, E.G., and Bertram, G.T., 1993. Carbonate concepts from the Maldives, Indian Ocean. *AAPG Studies in Geology,* 34. **http://archives.datapages.com/data/specpubs/carbona1/data/a047/a047/0001/0000/0007.htm**

Rao, T.H., 2001. Gas hydrate investigations along the continental margins of India [Ph.D. thesis]. Osmania University, Hyderabad.

Rea, D.K., 1992. Delivery of Himalayan sediment to the northern Indian Ocean and its relation to global climate, sea level, uplift, and seawater strontium. *In* Duncan, R.A., Rea, D.K., Kidd, R.B., von Rad, U., and Weissel, J.K. (Eds.), *Synthesis of Results from Scientific Drilling in the Indian Ocean.* Geophysical Monograph, 70:387–402. **http://dx.doi.org/10.1029/GM070p0387**

Reijmer, J.J.G., Bauch, T., and Schäfer, P., 2012. Carbonate facies patterns in surface sediments of upwelling and non-upwelling shelf environments (Panama, East Pacific). *Sedimentology,* 59(1):32–56. **http://dx.doi.org/10.1111/j.1365-3091.2010.01214.x**

Rio, D., Fornaciari, E., and Raffi, I., 1990. Late Oligocene through early Pleistocene calcareous nannofossils from western equatorial Indian Ocean (Leg 115). *In* Duncan, R.A., Backman, J., Peterson, L.C., et al., *Proceedings of the Ocean Drilling Program, Scientific Results,* 115: College Station, TX (Ocean Drilling Program), 175–235. **http://dx.doi.org/10.2973/odp.proc.sr.115.152.1990**

Ruddiman, W.F., 2006. What is the timing of orbital-scale monsoon changes? *Quaternary Science Reviews,* 25(7–8):657–658. **http://dx.doi.org/10.1016/j.quascirev.2006.02.004**

Sattler, U., Immenhauser, A., Schlager, W., and Zampetti, V., 2009. Drowning history of a Miocene carbonate platform (Zhujiang Formation, South China Sea). *Sedimentary Geology,* 219(1–4):318–331. **http://dx.doi.org/10.1016/j.sedgeo.2009.06.001**

Shackleton, N.J., 1985. Oceanic carbon isotope constraints on oxygen and carbon dioxide in the Cenozoic atmosphere. *In* Sundquist, E.T., and Broecker, W.S. (Eds.), *The Carbon Cycle and Atmospheric* CO_2*: Natural Variations Archean to Present.* Geophysical Monograph, 32:412–417. **http://dx.doi.org/10.1029/GM032p0412**

Subrahmanyam, V., Gopala Rao, D., Ramprasad, T., Kamesh Raju, K.A., and Gangadhura Rao, M.G., 1991. Gravity anomalies and crustal structure of the western continental margin off Goa and Mulki, India. *Marine Geology,* 99(1–2):247–256. **http://dx.doi.org/10.1016/0025-3227(91)90094-K**

Swart, P.K., 2008. Global synchronous changes in the carbon isotopic composition of carbonate sediments unrelated to changes in the global carbon cycle. *Proceedings of the National Academy of Sciences of the United States of America,* 105(37):13741–13745. **http://dx.doi.org/10.1073/pnas.0802841105**

Tomczak, M., and Godfrey, J.S., 1994. *Regional Oceanography: An Introduction:* New York (Pergamon Press).

Veizer, J., Ala, D., Azmy, K., Bruckschen, P., Buhl, D., Bruhn, F., Carden, G.A.F., Diener, A., Ebneth, S., Godderis, Y., Jasper, T., Korte, C., Pawellek, F., Podlaha, O.G., and Strauss, H., 1999. $^{87}Sr/^{86}Sr$, $\delta^{13}C$ and $\delta^{18}O$ evolution of Phanerozoic seawater. C*hemical Geology,* 161(1–3):592–88. **http://dx.doi.org/10.1016/S0009-2541(99)00081-9**

Woodruff, F., and Savin, S.M., 1989. Miocene deepwater oceanography. *Paleoceanography,* 4(1):87–140. **http://dx.doi.org/10.1029/PA004i001p00087**

Xie, S.-P., Xu, H., Saji, N.H., Wang, Y., and Liu, W.T., 2006. Role of narrow mountains in large-scale organization of Asian monsoon convection. *Journal of Climate,* 19(14):3420–3429. **http://dx.doi.org/10.1175/JCLI3777.1**

Zachos, J., Pagani, M., Sloan, L., Thomas, E., and Billups, K., 2001. Trends, rhythms, and aberrations in global climate 65 Ma to present. *Science,* 292(5517):686–693. **http://dx.doi.org/10.1126/science.1059412**

Zampetti, V., Schlager, W., van Konijnenburg, J.-H., and Everts, A.-J., 2004. Architecture and growth history of a Miocene carbonate platform from 3D seismic reflection data: Luconia province, offshore Sarawak, Malaysia. *Marine and Petroleum Geology*, 21(5): 517–534. **http://dx.doi.org/10.1016/j.marpetgeo.2004.01.006**

Zheng, H., Powell, C.M., Rea, D.K., Wang, J., and Wang, P., 2004. Late Miocene and mid-Pliocene enhancement of the East Asian monsoon as viewed from the land and sea. *Global and Planetary Change*, 41(3–4):147–155. **http://dx.doi.org/10.1016/j.gloplacha.2004.01.003**

Zhisheng, A., Clemens, S.C., Shen, J., Qiang, X., Jin, Z., Sun, Y., Prell, W.L., Luo, J., Wang, S., Xu, H., Cai, Y., Zhou, W., Liu, X., Liu, W., Shi, Z., Yan, L., Xiao, X., Chang, H., Wu, F., Ai, L., and Lu, F., 2011. Glacial–interglacial Indian summer monsoon dynamics. *Science*, 333(6043):719–723. **http://dx.doi.org/10.1126/science.1203752**

Table T1. Seismic horizons overview and characteristics (Betzler et al., 2013a).

Horizon	Impedance contrast	Polarity	Age
Seabed	Strong	Positive	recent
bEPlio	Weak	Negative	late Miocene/Pliocene
MM5	Strong	Positive	middle/late Miocene
MM3	Unstable	Positive	middle Miocene
bSN13	Unstable	Negative	middle Miocene
E/MM	Strong	Positive	middle Miocene
bMMio	Unstable	Negative	early/middle Miocene
EM1	Unstable	Positive	early Miocene
PB2bO	Unstable	Positive	early Miocene
O/Ma	Strong	Positive	Oligocene/Miocene

Table T2. Expedition 359 sites.

Site	Latitude	Longitude	Sediment type	Coring strategy	Water depth (m)	Target penetration (mbsf)
MAL-01A	4.933109°	73.011320°	Carbonate ooze, chalk, inner-platform limestone	APC, XCB, RCB	512	1060
MAL-02A	4.933156°	73.027983°	Platform to slope chalk-ooze, drifts	APC, XCB, RCB	483	560
MAL-03A	4.933064°	73.071305°	Drifts (ooze to chalk)	APC, XCB	520	435
MAL-04B (ODP 716)	4.929444°	73.286776°	Drifts (ooze to chalk)	APC, XCB	536	554
MAL-05A	4.766388°	72.983889°	Carbonate ooze, chalk, inner-platform limestone, slope deposits	APC, XCB, RCB	380	420
MAL-06B Alternate	4.771096°	73.066848°	Drifts (ooze to chalk)	APC, XCB	379	604
MAL-07A	4.766388°	73.135556°	Drifts (ooze to chalk)	APC, XCB	419	642
KK-03A Alternate Pending EPSP approval	15.3061°	70.9032°	Nannofossil and foraminifer oozes	APC, XCB	2685	450
KK-03B Pending EPSP approval	15.034617°	71.026561°	Nannofossil and foraminifer oozes	APC, XCB	2400	450

Table T3. Operations and time estimates for primary sites, Expedition 359.

Site	Location (Latitude Longitude)	Seafloor depth (mbrf)	Operations description	Transit (days)	Drilling/ coring (days)	Wireline log (days)
Darwin, Australia			**Begin Expedition** 5.0	Port Call Days		
			Transit ~3567 nmi from Darwin to Male @ 10.5 knots	14.0		
Male, Maldives			**Clear into Maldives** 0.5	Port Call Days		
			Transit ~49 nmi from Male to Site MAL-07A @ 10.5 knots	0.3		
MAL-07A	4°45.9833'N	430	Hole A: APC to 200 mbsf		1.0	
EPSP-710 mbsf	73°8.1334'E		Hole B: APC to 200 mbsf		0.6	
			Hole C: APC to 200 mbsf; XCB to 642 mbsf & wireline log		2.5	1.4
			(with triple combo, FMS-sonic, & VSI)			
			Subtotal Days On-site: 5.5			
			Transit ~9.0 nmi from Site MAL-07A to Site MAL-05A @ 10.5 knots	0.1		
MAL-05A	4°45.9833'N	391	Hole A: APC/XCB to 170 mbsf		0.7	
EPSP-420 mbsf	72°59.0333'E		Hole B: Drill; RCB to 420 mbsf & wireline log		1.7	0.9
			(with triple combo & FMS-sonic)			
			Subtotal Days On-site: 3.3			
			Transit ~11.3 nmi from Site MAL-05A to Site MAL-03A @ 10.5 knots	0.1		
MAL-03A	4°55.9838'N	531	Hole A: APC to 200 mbsf		0.8	
EPSP-532 mbsf	73°4.2783'E		Hole B: APC to 200 mbsf		0.5	
			Hole C: APC to 200 mbsf; XCB to 435 mbsf & wireline log		1.4	0.9
			(with triple combo & FMS-sonic)			
			Subtotal Days On-site: 3.6			
			Transit ~2.6 nmi from Site MAL-03A to Site MAL-02A @ 1.0 knots	0.1		
MAL-02A	4°55.9894'N	494	Hole A: APC to 200 mbsf; XCB to 325 mbsf		1.2	
EPSP-560 mbsf	73°1.6790'E					
			Subtotal Days On-site: 1.2			
			Transit ~1.0 nmi from Site MAL-02A to Site MAL-01A @ 1.0 knots	0.0		
MAL-01A	4°55.9865'N	523	Hole A: APC to 80 mbsf		0.4	
EPSP-1060 mbsf	73°0.6792'E		Hole B: Drill down to 80 mbsf and RCB to 1060 mbsf & wireline log		5.8	1.9
			(wireline log with triple combo, FMS-sonic, & VSI)			
			Subtotal Days On-site: 8.1			
			Transit ~1.0 nmi from Site MAL-01A to Site MAL-02A @ 1.0 knots	0.0		
MAL-02A	4°55.9894'N	494	Hole B: Drill; RCB to 560 mbsf & wireline log		2.0	0.9
EPSP-560 mbsf	73°1.6790'E		(with triple combo & FMS-sonic)			
			Subtotal Days On-site: 2.9			
			Transit ~15.5 nmi from Site MAL-02A to Site MAL-04B @ 10.5 knots	0.1		
MAL-04B	4°55.7664'N	547	Hole A: Drill/wash to 170 mbsf (already cored at ODP Site 716)		2.2	1.0
(ODP 716)	73°17.2066'E		APC/XCB to 554 mbsf & wireline log			
EPSP-590 mbsf			(with triple combo, FMS-sonic, & VSI)			
			Subtotal Days On-site: 3.2			
			Transit ~66 nmi from Site MAL-04B to Male @ 10.5 knots	0.3		
Male, Maldives			**Clear out of Maldives** 0.5	Port Call Days		
			Transit ~687 nmi from Male to Site KK-03 @ 10.5 knots	2.7		
KK-03B	15°2.0770'N	2411	Hole A: APC to 200 mbsf; XCB to 450 mbsf		2.8	
Waiting on	71°1.5937'E		Hole B: APC to 200 mbsf; XCB to 450 mbsf		2.4	
EPSP approval			Hole C: APC to 200 mbsf		1.4	
			Subtotal Days On-site: 6.6			
			Transit ~730 nmi from Site KK-03 to Colombo @ 10.5 knots	2.9		
Colombo, Sri Lanka			**End Expedition**	20.6	27.4	7

Port Call:	6.0	Total Operating Days:	55.0
Subtotal On-site:	34.4	Total Expedition:	61.0

Seafloor depth corrected to rig floor dual elevator stool or meters below rig floor (mbrf).

Table T4. Operations and time estimates for alternate sites, Expedition 359.

Site	Location (Latitude Longitude)	Seafloor depth (mbrf)	Operations description	Transit (days)	Drilling/ coring (days)	Wireline log (days)
MAL-06B	4° 46.2658' N	390	Hole A: APC to 200 mbsf		0.7	
EPSP-604 mbsf	73° 4.0109' E		Hole B: APC to 200 mbsf		0.4	
			Hole C: APC to 200 mbsf; XCB to 604 mbsf and wireline log		2.1	1.0
			(triple-combo and FMS-sonic)			
			Subtotal days on site 4.2			
				2.5		
KK-03A	15.3061° N	2685	Hole A: APC to 200 mbsf		1.4	
EPSP-951 mbsf	70.9032° E		Hole B: APC to 200 mbsf; XCB to 400 mbsf		2.4	
Waiting on			Hole C: APC to 200 mbsf; XCB to 400 mbsf		2.8	
EPSP approval						
			Subtotal days on site 6.6			

Seafloor depth corrected to rig floor dual elevator stool or meters below rig floor (mbrf).

Figure F1. Location of Maldives and Expedition 359 proposed drill sites in the Indian Ocean.

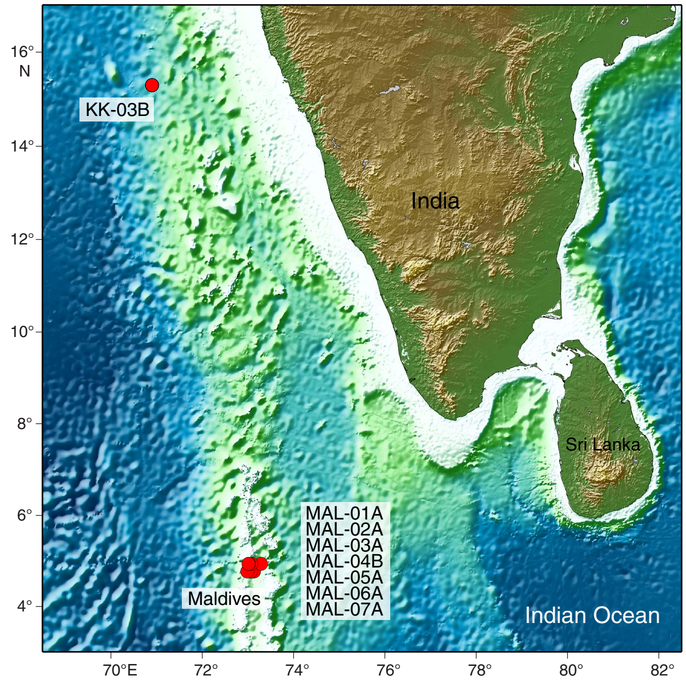

Figure F2. A. Location map of the Maldives in the central equatorial Indian Ocean. **B.** Expedition 359 study area. **C.** M95 NEOMA cruise high-resolution seismic line and wells drilled in the Maldives.

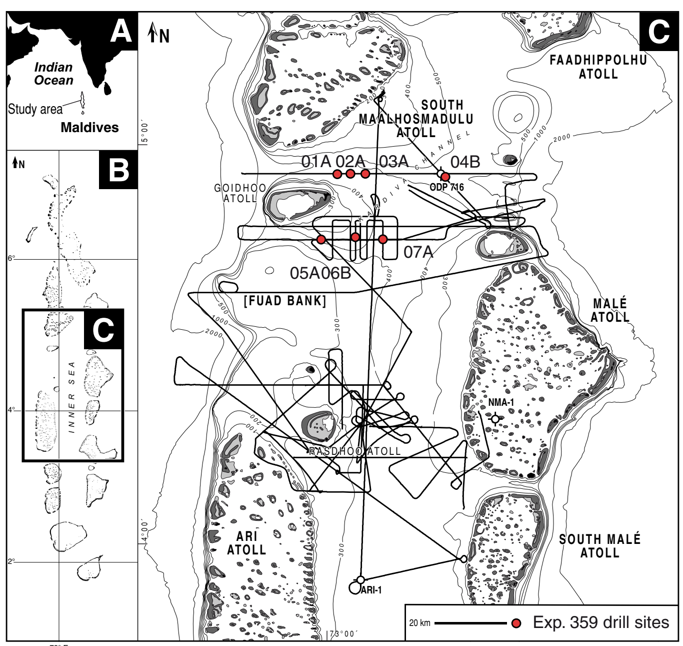

Figure F3. Top: well-to-seismic tie for establishment of chronostratigraphic framework. Age, biostratigraphy, gamma ray log, and lithology columns are taken from industry Well ARI-1 (modified after Belopolsky and Droxler, 2004a). Depth conversion of seismic Line NEOMA-P7 was done using an irregular spaced velocity log from Well ARI-1. High-resolution seismics are displayed in red to yellow and blue to turquoise colors corresponding to changes in peak and trough amplitudes, respectively (SEG normal polarity). Shell seismic line after Belopolsky and Droxler (2004b). Bottom: west–east crossing seismic Line NEOMA-P7 (vertical exaggeration = 25×) with Well ARI-1 (cf. Figure **F1**). 1 = Eocene, 2 = early Oligocene, 3 = late Oligocene, 4 = early Miocene, 5 = middle Miocene, 6 = late Miocene, 7 = Pliocene–Pleistocene (Betzler et al., 2013).

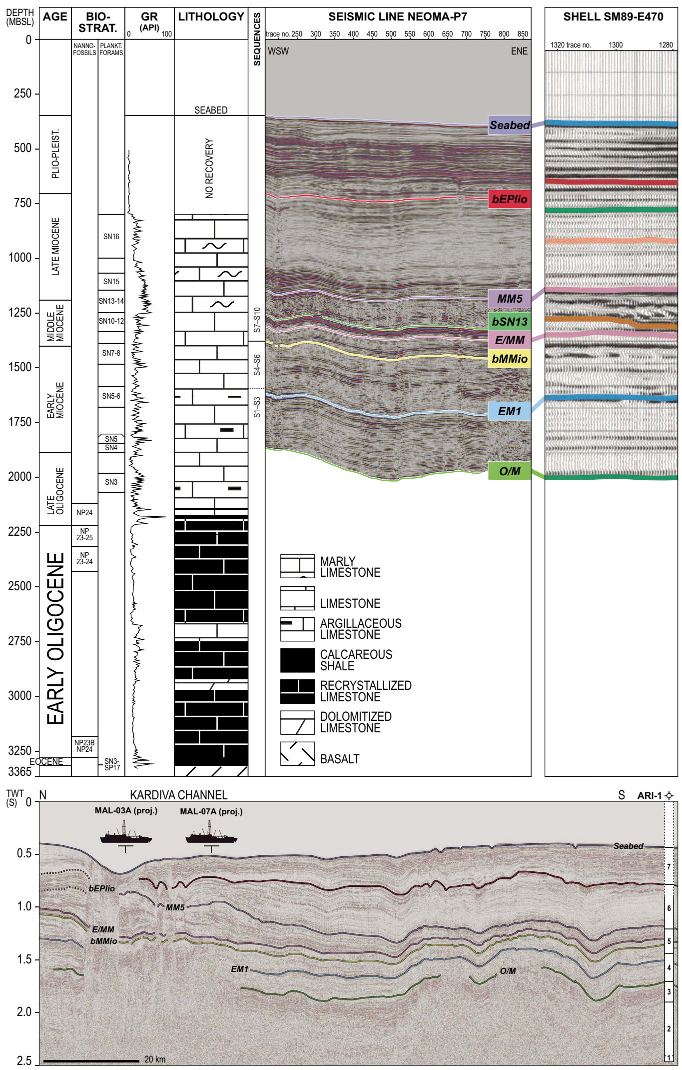

Figure F4. A. Published seismic units in the Maldives carbonate edifice: N1–N5, PP from Aubert and Droxler (1996) and E-Mio 1/2, M1–M5, L-Mio 1–LP-P according to Belopolsky and Droxler (2004b). **B.** Seismic Line NEOMA-P65 (vertical exaggeration = 20×) runs west–east along the South Maalhosmadulu and Goidhoo interatoll channel and crosscuts Kardiva Channel (cf. Figure **F1**). **C.** General interpretation from high-resolution seismic data for this study (Betzler et al., 2013a). I = upper Miocene, II = lower Pliocene, III = middle Pliocene, IV = upper Pliocene, V = Pleistocene.

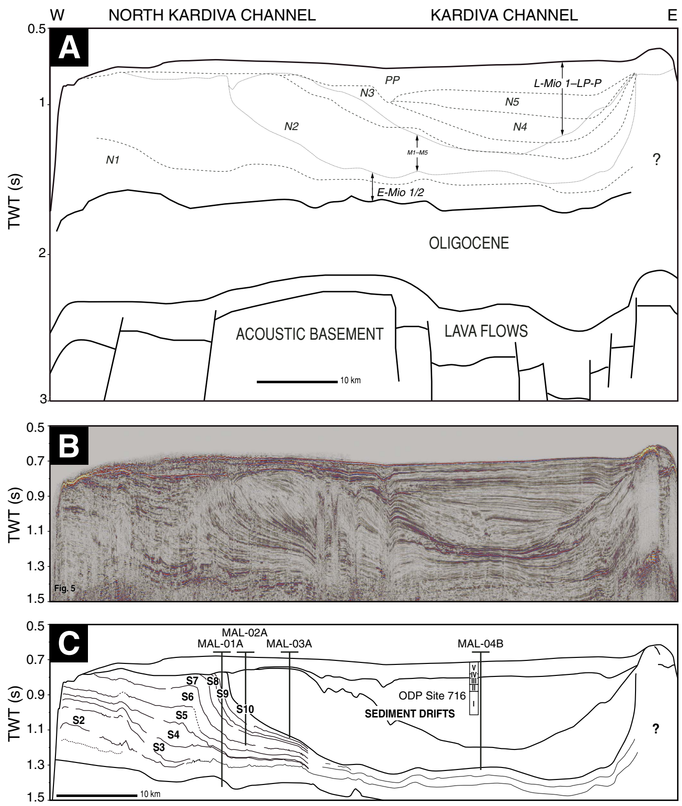

Figure F5. **A.** Close view of the western part of seismic Line NEOMA-P65 (vertical exaggeration = 7.5×) running west–east through northern Kardiva Channel. **B.** Interpretation (Betzler et al., 2013a). S1–S10 and SB1–SB10 refer to sequences and sequence boundaries, respectively. Black line = bank edge growth path.

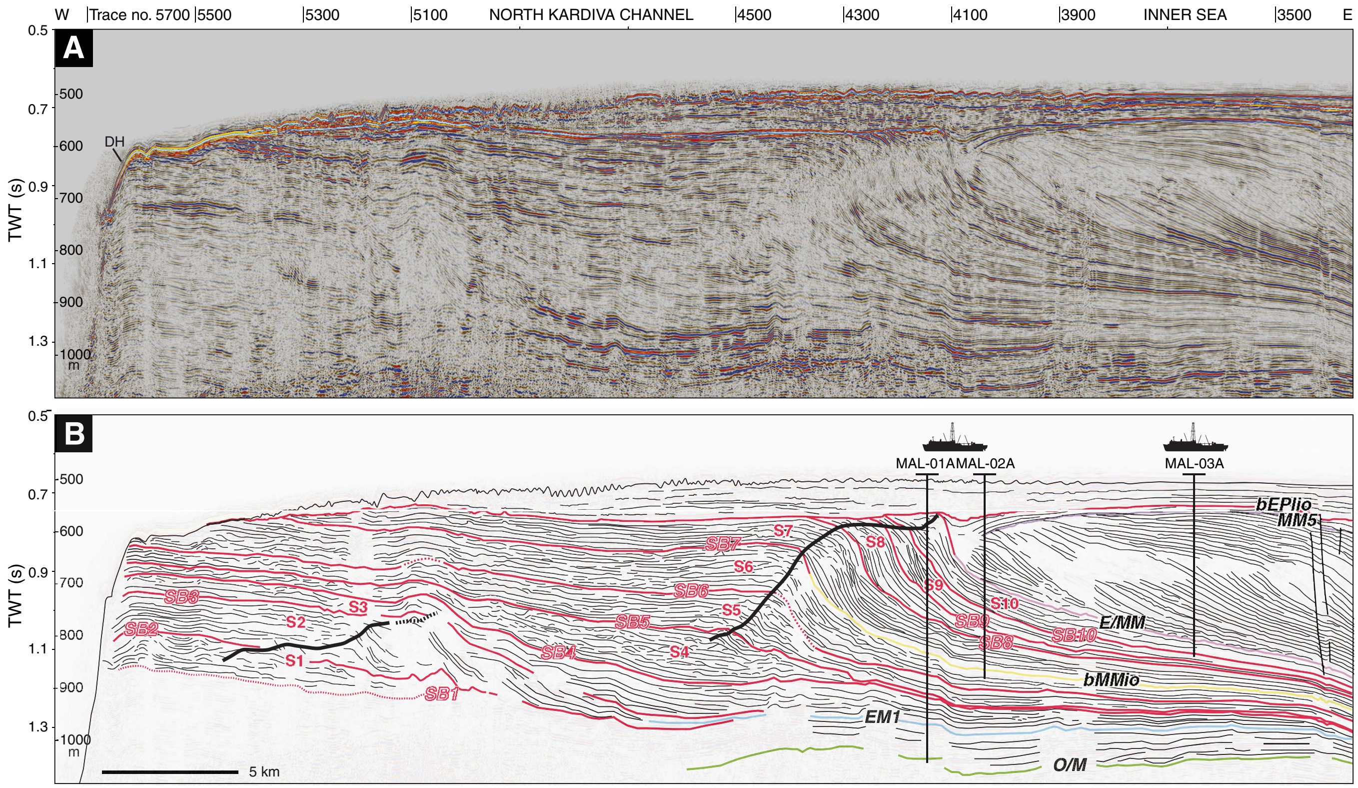

Figure F6. Seismic Line 65 crossing the northern part of the Maldives from the northwest to northeast Kardiva Channel (Lüdmann et al., 2013). Shown are the mapped 9 post-late middle Miocene megaunits and the location of ODP Site 716. CB = carbonate bank.

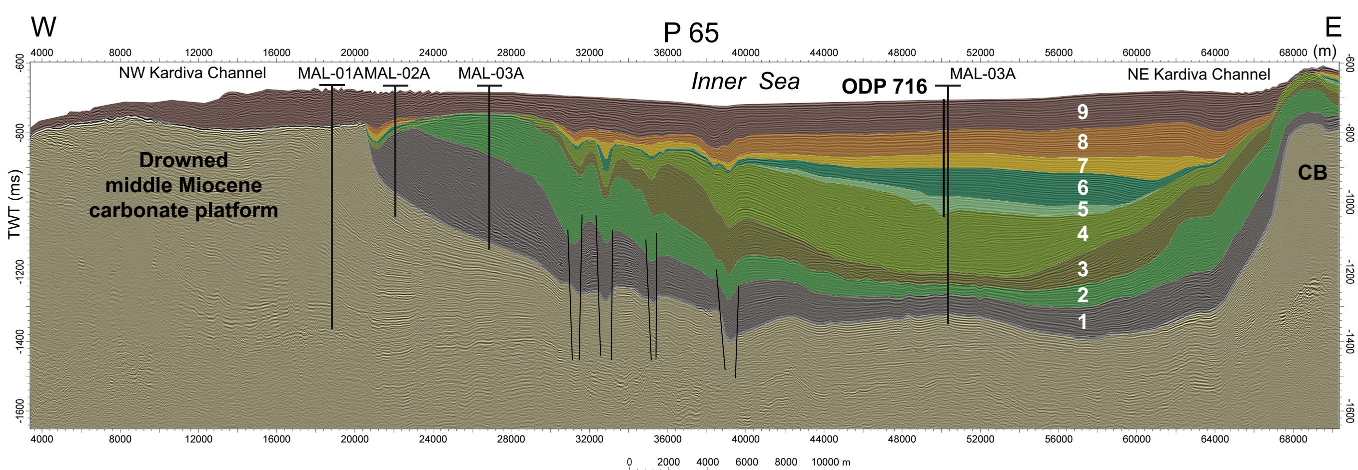

Figure F7. A. Central part of Profile 65 showing the sediment waves in the distal area of Units 3 and 4. **B.** Percentage of the <63 µm fraction in the cores collected at ODP Site 716 (Lüdmann et al., 2013).

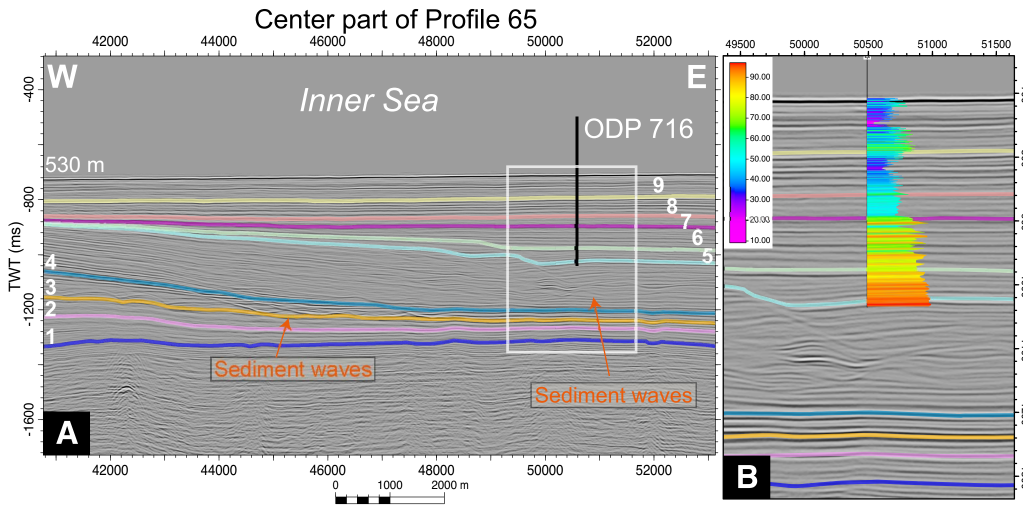

Figure F8. Sketch of the Neogene stratigraphy of the Maldives showing the stratigraphic relationship between drowned parts of the archipelago, drift deposits, and still-active atolls (after Betzler et al., 2013a). Expedition 359 sites are located to recover the bank-interior and slope deposits of the drowned banks, the platform-to-drift turnover, and the drift succession.

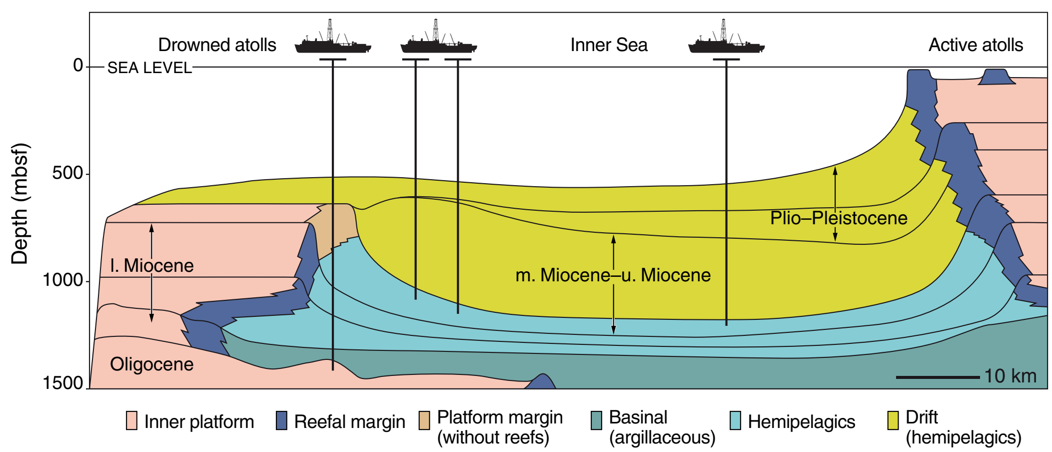

Figure F9. Location of Sites KK-3B and NGHP 01-1A with the total thickness of sediments in the Konkan Kerala Basin (after Campanille et al., 2008).

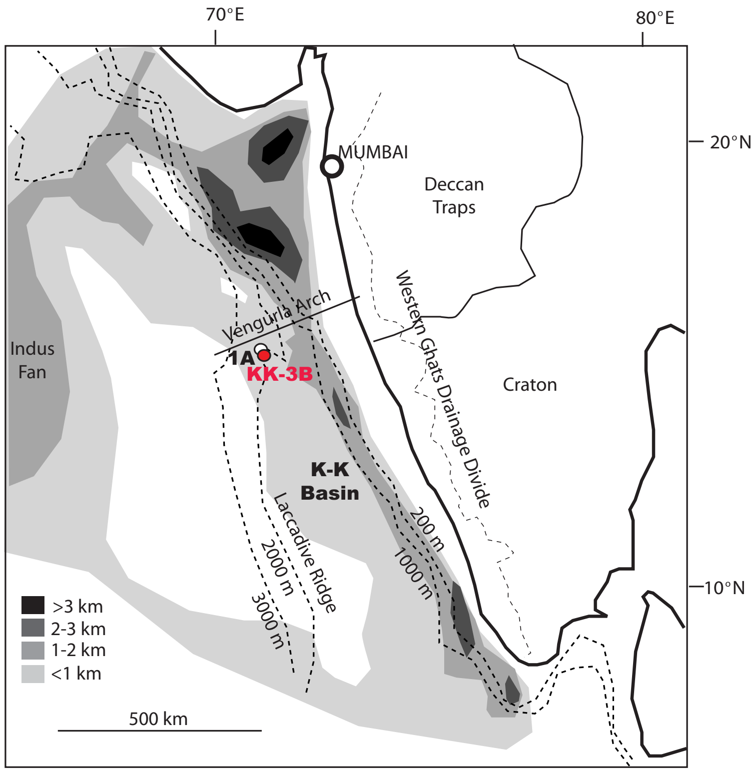

Figure F10. Location and bathymetry for Site KK-3B (2400 m water depth).

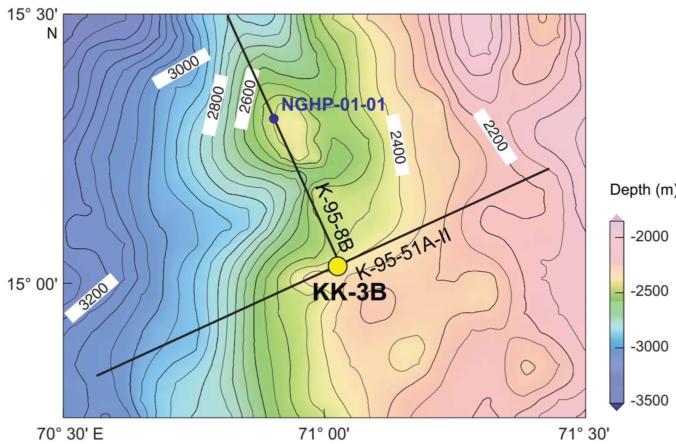

Figure F11. Along-strike and dip seismic profiles for Site KK-3B. Estimated ages of horizons are shown.

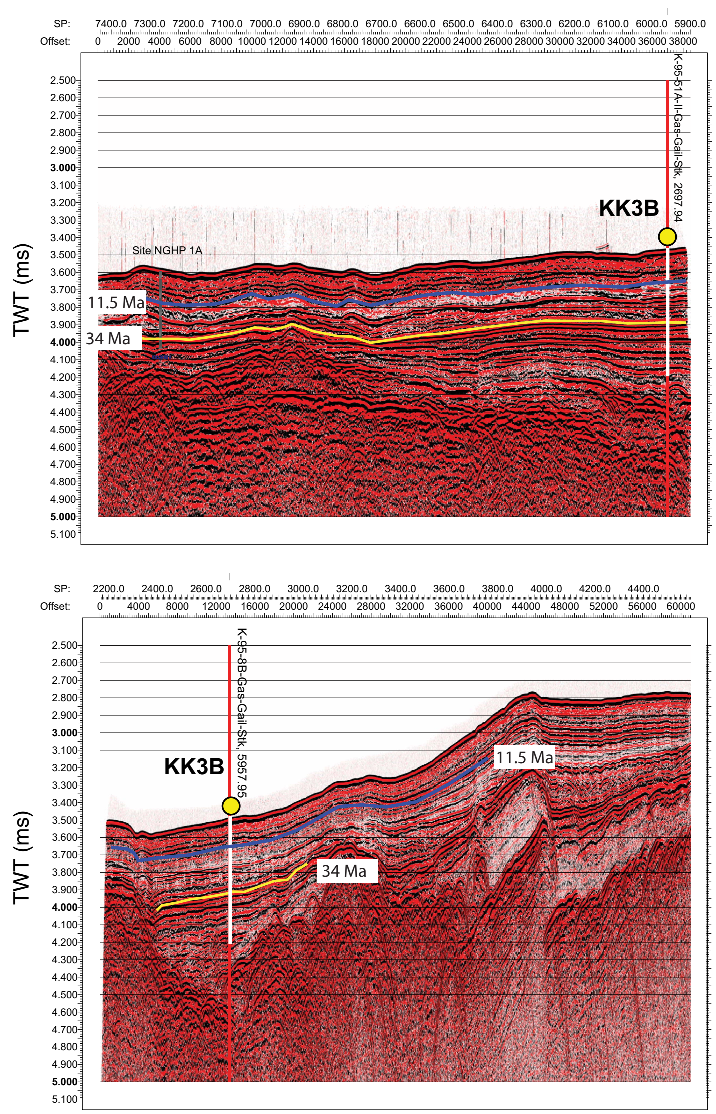

Figure F12. Simplified lithology log and a proxy for terrigenous flux-scanning XRF Ti/Ca for Site KK-3B.

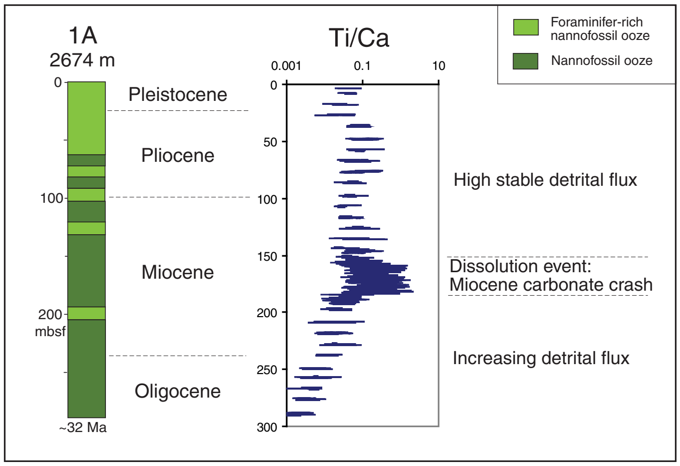

Figure F13. Bathymetric and site track map, Sites MAL-07A, MAL-06B, and MAL-05A.

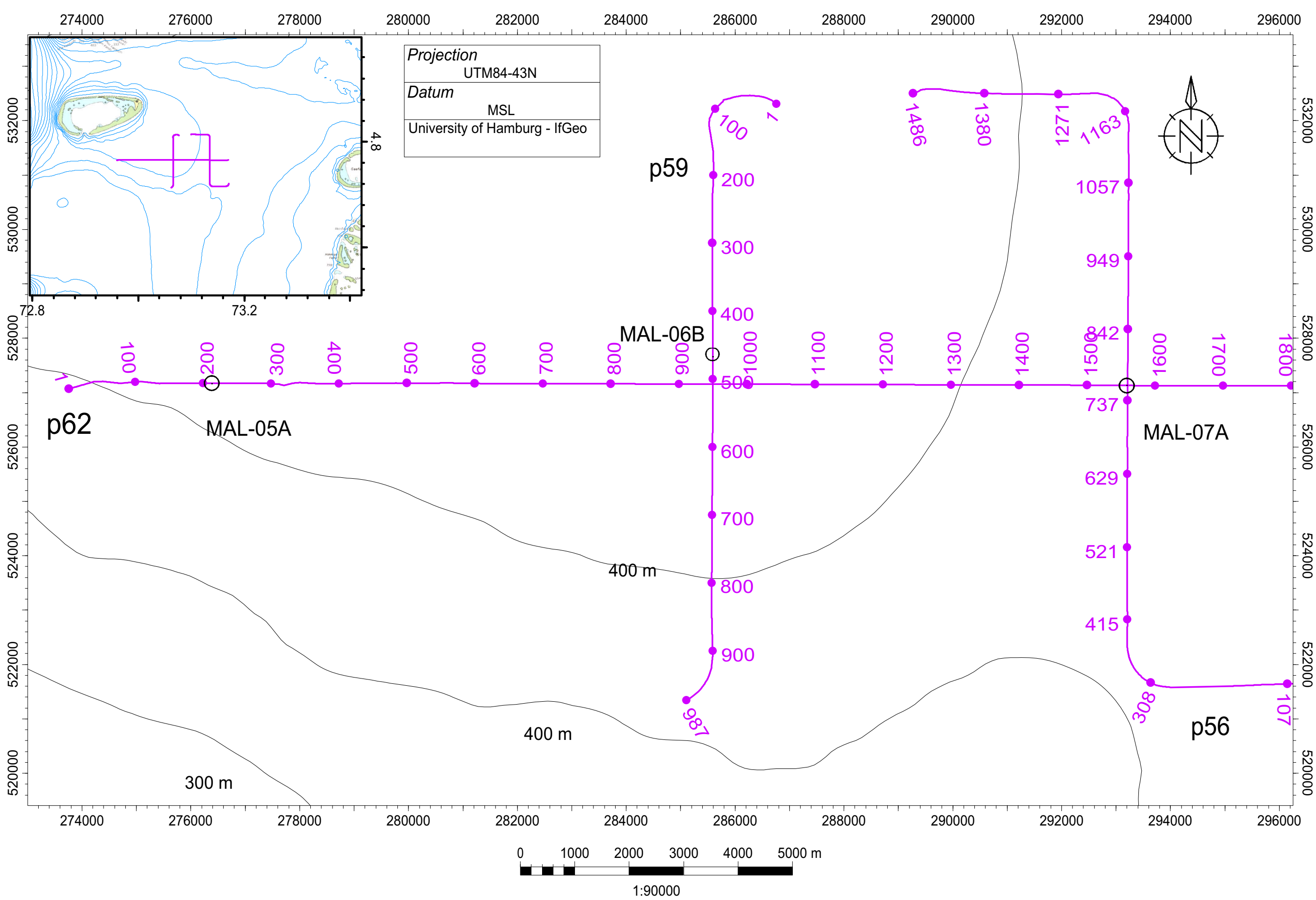

Figure F14. Primary seismic Line 62 (Site MAL-07A).

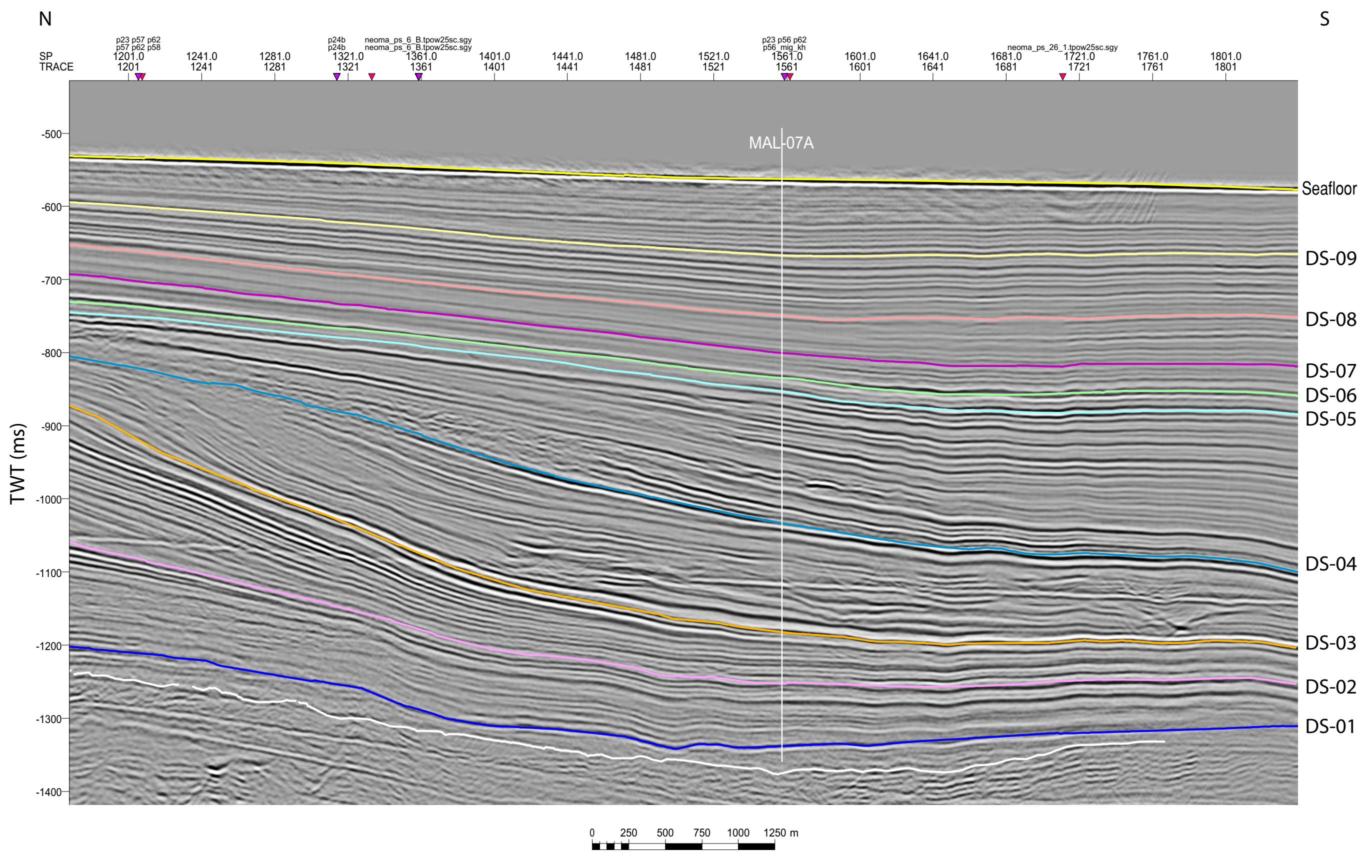

Figure F15. Primary seismic Line 59 (Site MAL-06B).

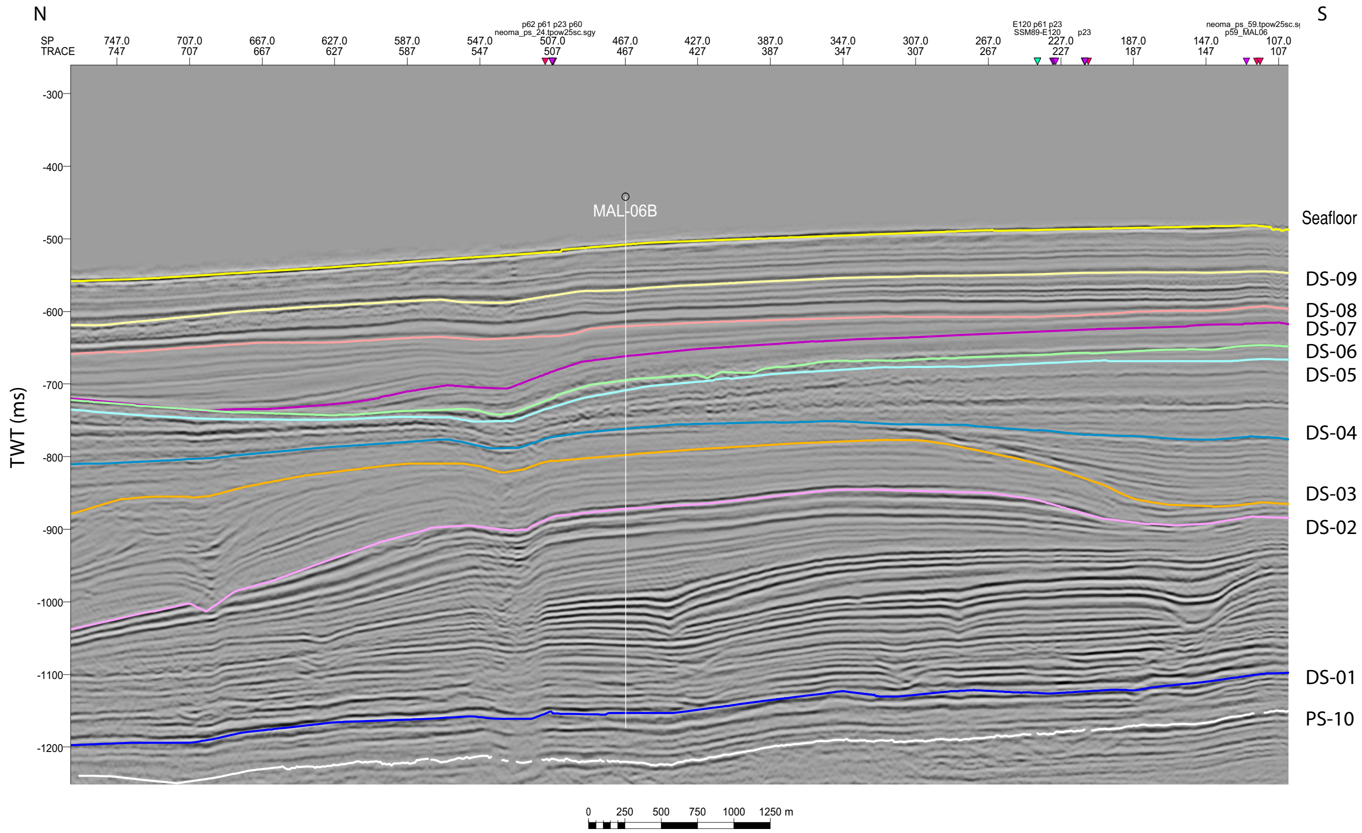

Figure F16. Primary seismic Line 62 (Site MAL-05A).

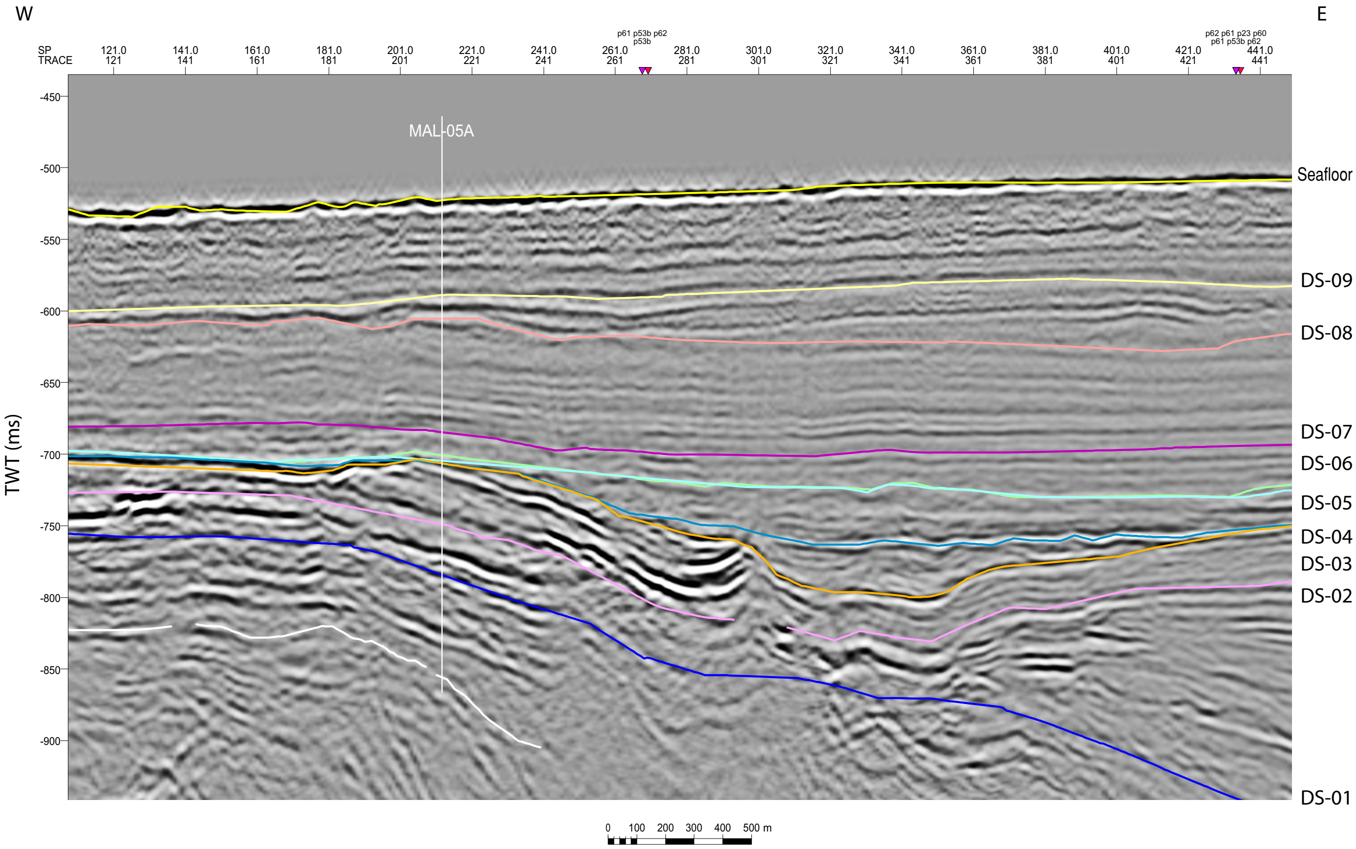

Figure F17. Bathymetric and site track map, Site MAL-04B.

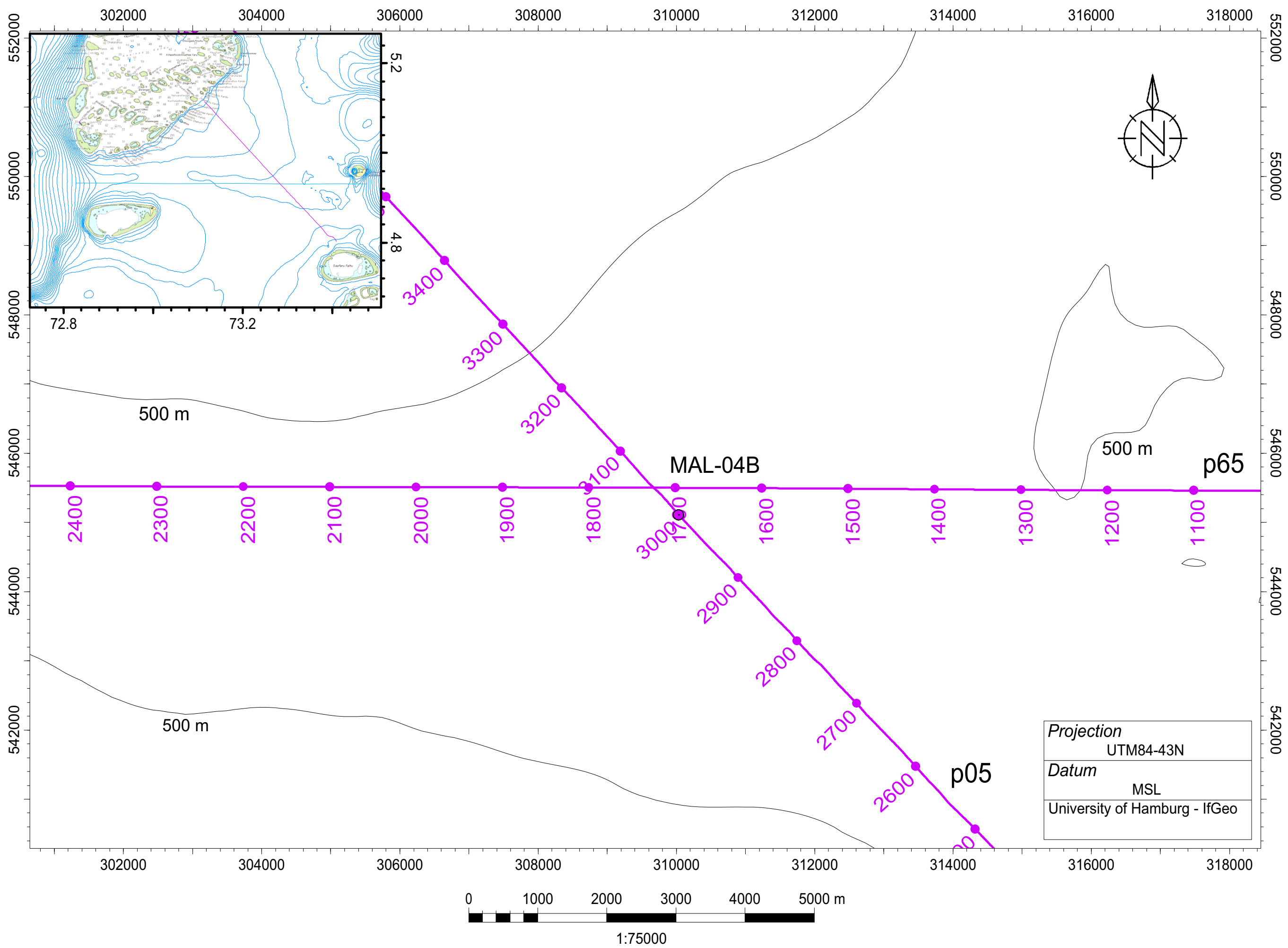

Figure F18. Primary seismic Line 65 (Site MAL-04B).

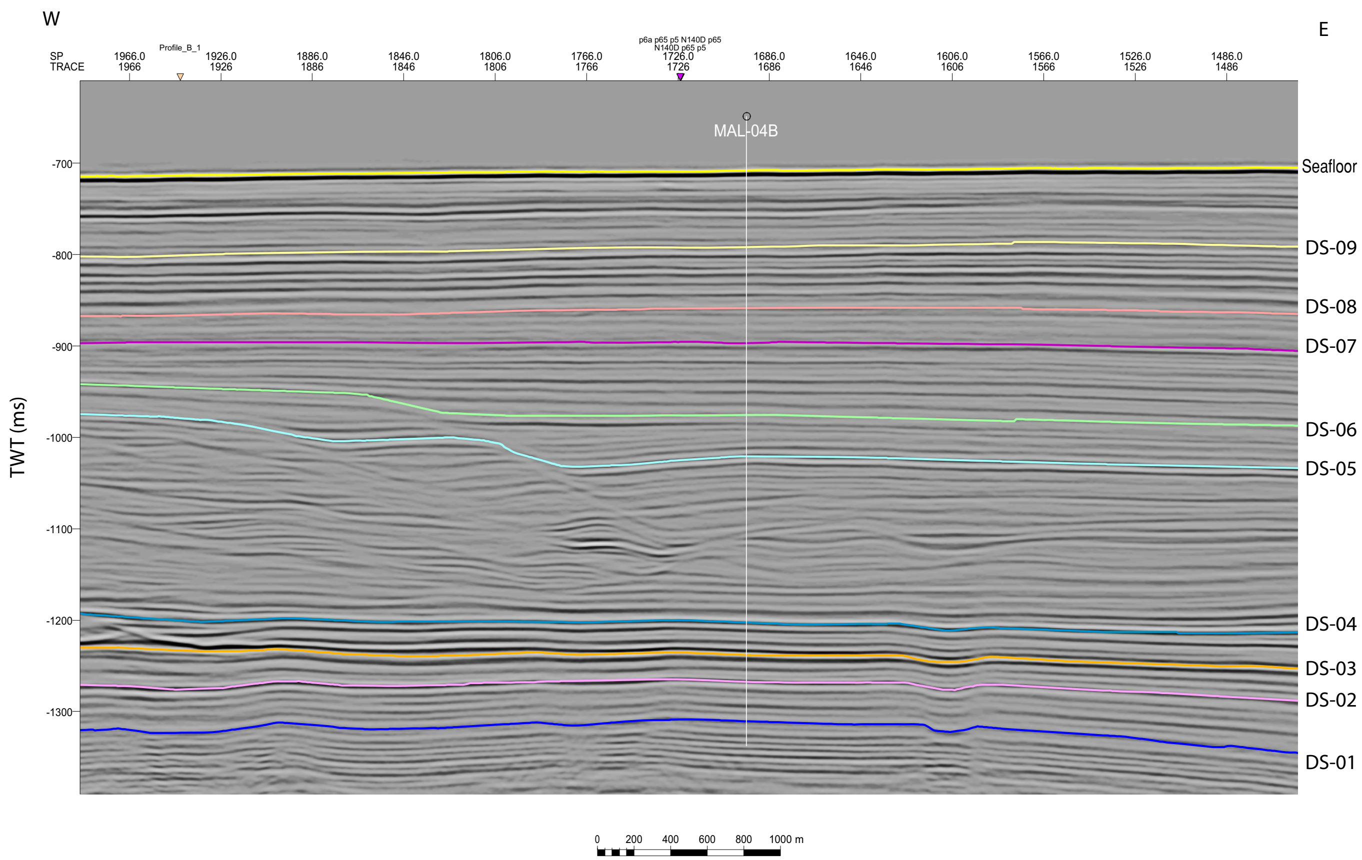

Figure F19. Bathymetric and site track map, Sites MAL-01A, MAL-02A and MAL-03A.

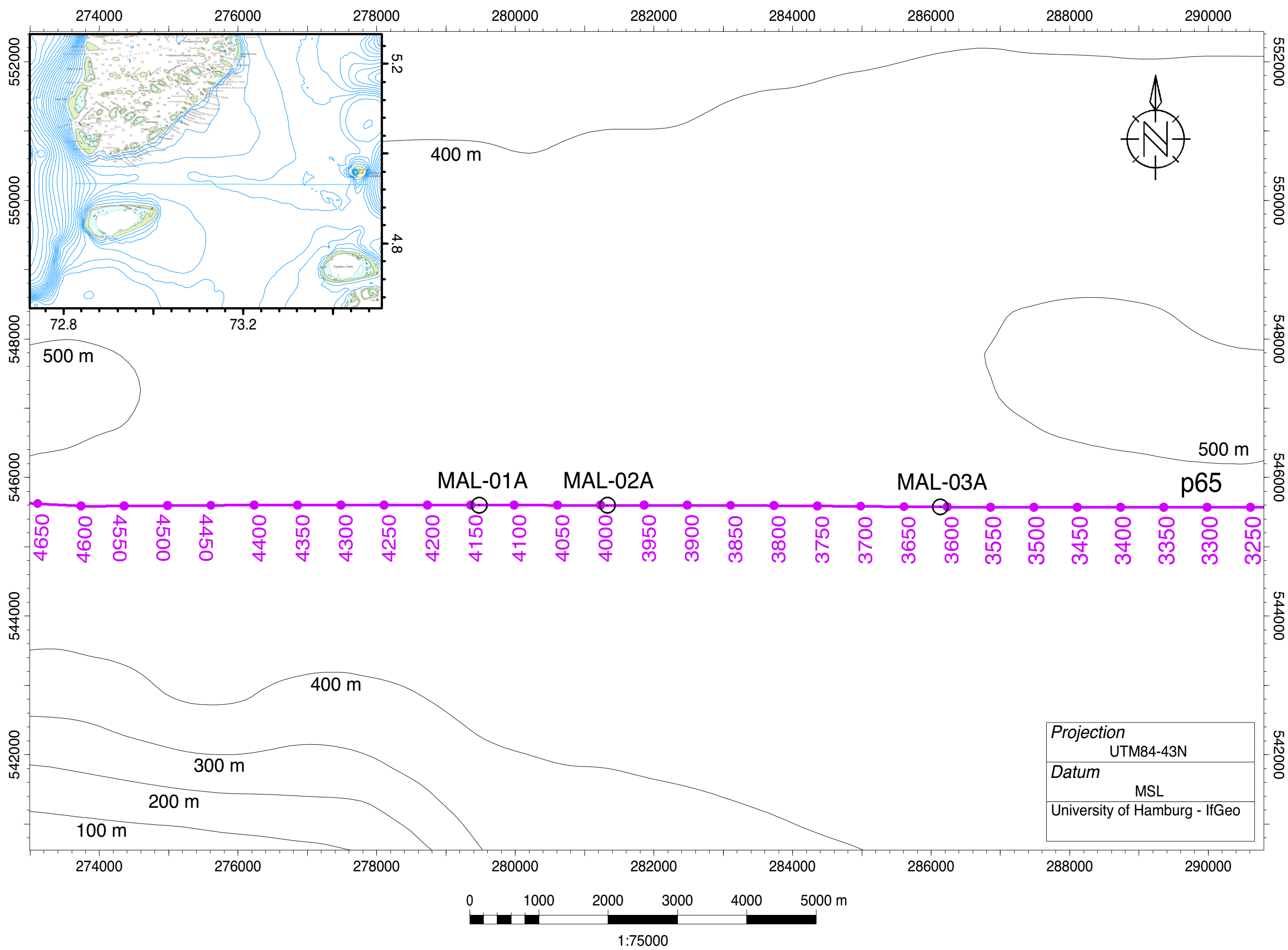

Figure F20. Primary seismic Line 65 (Sites MAL-02A and MAL-03A).

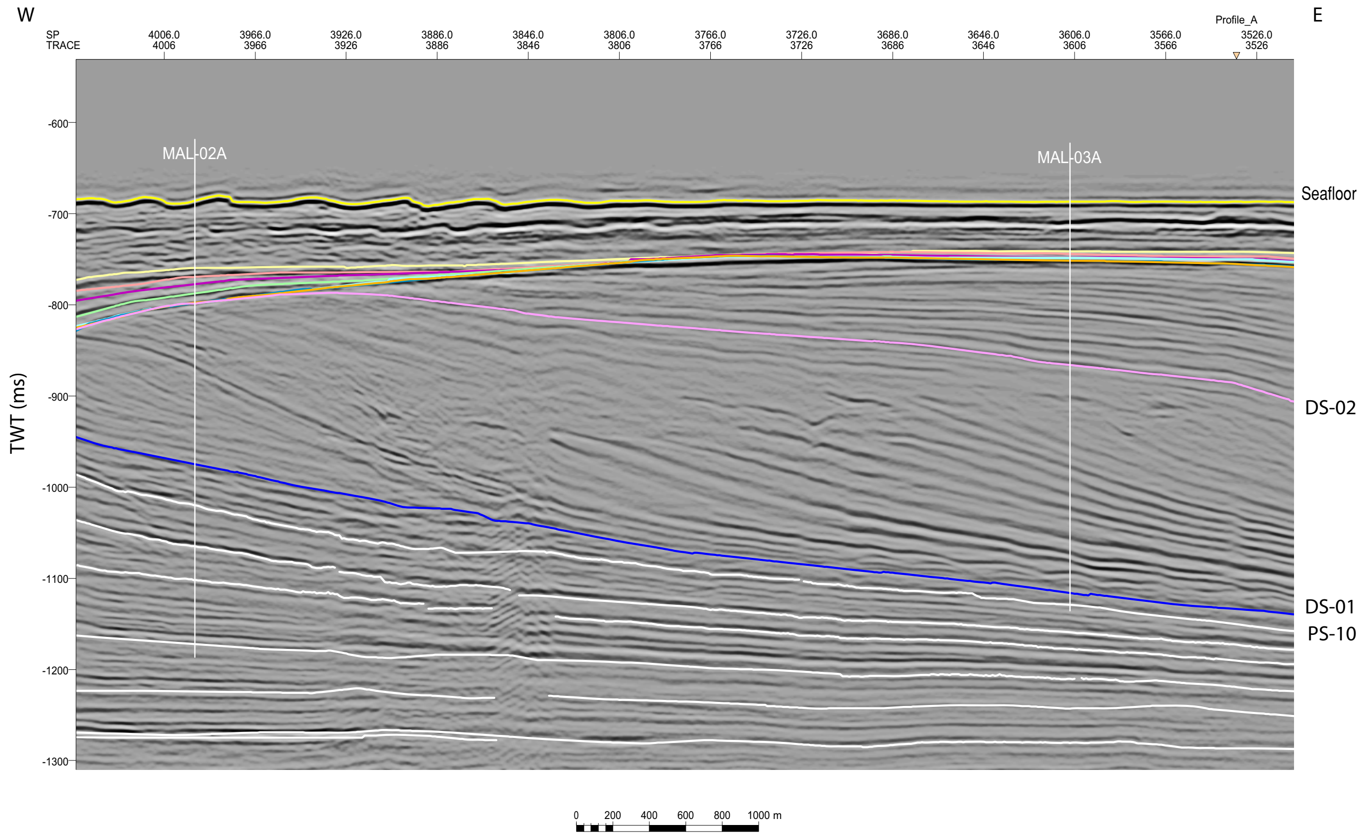

Figure F21. Primary seismic Line 65 (Sites MAL-01A and MAL-02A).

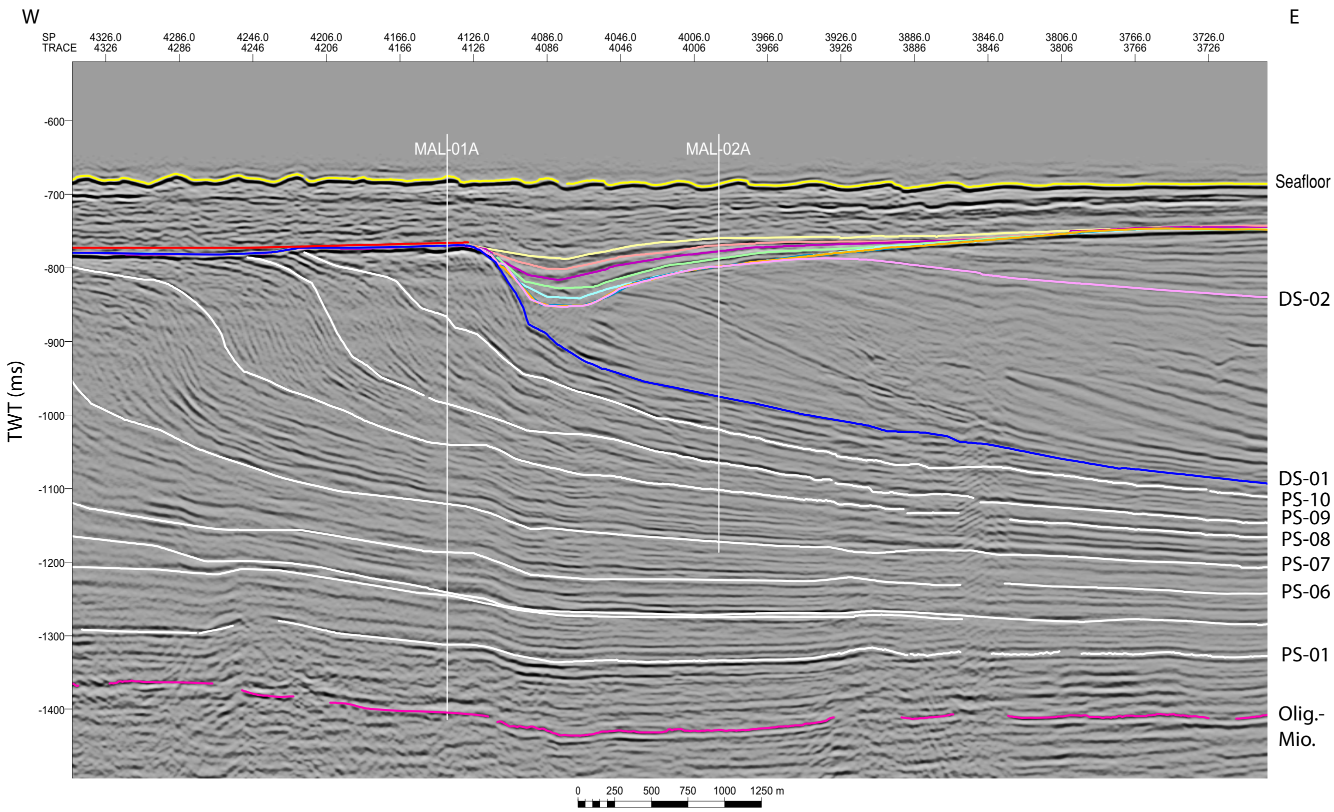

Site summaries

Site MAL-07A

Priority:	Primary
Position:	4.766388°N, 73.135556°E
Jurisdiction:	Maldives
Water depth (m):	419
Target drilling depth (mbsf):	642
Approved maximum penetration (mbsf):	710
Survey coverage (track map; seismic profile):	• Location map (Fig. **F13**) • Primary line(s): 124-channel seismic Line 62 (Fig. **F14**) • 124-channel seismic Line 59
Objective(s):	1. Analyze cyclostratigraphy of drift deposits, providing reconstructions of changes in the current regime and monsoon cyclicity 2. Constrain the timing of unconformities and sedimentary interruptions
Drilling program:	Triple APC to 200 mbsf APCT-3 measurements and orientation on all holes Hole C: XCB to ~642 mbsf
Logging and downhole measurement program:	Wireline log with triple combo, FMS-sonic, and VSI.
Nature of rock anticipated:	Calcareous ooze, chalk

Site summaries (continued)

Site MAL-06B

Priority:	Alternate
Position:	4.771096°N, 73.066848°E
Jurisdiction:	Maldives
Water depth (m):	379
Target drilling depth (mbsf):	604
Approved maximum penetration (mbsf):	604
Survey coverage (track map; seismic profile):	Location map (Fig. **F13**) Primary line(s): Line 59 (Fig. **F15**)
Objective(s):	1. Analyze cyclostratigraphy of drift deposits, providing reconstructions of changes in the current regime and monsoon cyclicity 2. Provide a detailed reconstruction of the predrowning, drowning, and postdrowning evolution of the carbonate bank by linking the seismic stratigraphic record to the sedimentary record 3. Constrain the timing of this evolution, allowing age assignments of unconformities, sedimentary interruptions, sedimentary turnovers, and onset of drift deposition 4. Reconstruct and date bank to drift turnover
Drilling program:	Triple APC to 200 mbsf Hole C: XCB to 604 mbsf
Logging and downhole measurement program:	Wireline log with triple combo and FMS-sonic
Nature of rock anticipated:	Calcareous ooze, chalk (drifts)

Site summaries (continued)

Site MAL-05A

Priority:	Primary
Position:	4.766388°N, 72.983889°E
Jurisdiction:	Maldives
Water depth (m):	380
Target drilling depth (mbsf):	420
Approved maximum penetration (mbsf):	420
Survey coverage (track map; seismic profile):	Location map (Fig. F13) Primary line(s): Line 62 (Fig. F16)
Objective(s):	1. Provide detailed reconstruction of the predrowning, drowning, and postdrowning evolution of the carbonate bank by linking the seismic stratigraphic record to the sedimentary record 2. Constrain the timing of this evolution, allowing age assignments of unconformities, sedimentary interruptions, sedimentary turnovers, and onset of drift deposition 3. Reconstruct and date bank to drift turnover
Drilling program:	Single APC/XCB to ~170 mbsf (based on seismic). Hole A: orientation and APCT-3 measurements Hole B: drill to ~170 with RCB and center bit and with RCB to 420 mbsf
Logging and downhole measurement program:	Wireline log with triple combo and FMS-sonic
Nature of rock anticipated:	Calcareous ooze, chalk, limestone

Site MAL-04B

Priority:	Primary
Position:	4.929444°N, 73.286776°E
Jurisdiction:	Maldives
Water depth (m):	533
Target drilling depth (mbsf):	554
Approved maximum penetration (mbsf):	590
Survey coverage (track map; seismic profile):	ODP Site 716 Location map (Fig. F17) Primary line(s): Line 65 (Fig. F18)
Objective(s):	1. Analyze cyclostratigraphy of drift deposits, providing reconstructions of changes in the current regime and monsoon cyclicity 2. Constrain the timing of unconformities and sedimentary interruptions
Drilling program:	Hole A: drill/wash to 170 mbsf, APC/XCB to 554 mbsf
Logging and downhole measurement program:	Wireline log with triple combo, FMS-sonic, and VSI
Nature of rock anticipated:	Calcareous ooze, chalk

Site summaries (continued)

Site MAL-03A

Priority:	Primary
Position:	4.933064°N, 73.071305°E
Jurisdiction:	Maldives
Water depth (m):	520
Target drilling depth (mbsf):	435
Approved maximum penetration (mbsf):	532
Survey coverage (track map; seismic profile):	Location map (Fig. F19) Primary line(s): Line 65 (Fig. F20)
Objective(s):	1. Analyze cyclostratigraphy of drift deposits, providing reconstructions of changes in the current regime and monsoon cyclicity 2. Constrain the timing of unconformities and sedimentary interruptions
Drilling program:	Triple APC to 200 mbsf Hole A: APCT-3 measurements and orientation Hole C: XCB to ~435 mbsf
Logging and downhole measurement program:	Wireline log with triple combo and FMS-sonic
Nature of rock anticipated:	Calcareous ooze, chalk, limestone

Site MAL-02A

Priority:	Primary
Position:	4.933156°N, 73.027983°E
Jurisdiction:	Maldives
Water depth (m):	483
Target drilling depth (mbsf):	560
Approved maximum penetration (mbsf):	560
Survey coverage (track map; seismic profile):	Location map (Fig. F19) Primary line(s): Line 65 (Fig. F21)
Objective(s):	1. Provide detailed reconstruction of the predrowning, drowning, and postdrowning evolution of the carbonate bank by linking the seismic stratigraphic record to the sedimentary record 2. Constrain the timing of this evolution, allowing age assignments of unconformities, sedimentary interruptions, sedimentary turnovers, and onset of drift deposition 3. Reconstruct and date bank to drift turnover
Drilling program:	Single APC hole to 200 mbsf and then XCB to 325 mbsf Hole A: APCT-3 measurements and orientation Hole B: drill to ~320 mbsf, RCB to 560 mbsf
Logging and downhole measurement program:	Wireline log with triple combo and FMS-sonic
Nature of rock anticipated:	Calcareous ooze, chalk, possibly limestone

Site summaries (continued)

Site MAL-01A

Priority:	Primary
Position:	4.933109°N, 73.011323°E
Jurisdiction:	Maldives
Water depth (m):	512
Target drilling depth (mbsf):	1060
Approved maximum penetration (mbsf):	1060
Survey coverage (track map; seismic profile):	Location map (Fig. F19) Primary line(s): Line 65 (Fig. F21)
Objective(s):	1. Provide detailed reconstruction of the predrowning, drowning, and postdrowning evolution of the carbonate bank by linking the seismic stratigraphic record to the sedimentary record 2. Constrain the timing of this evolution, allowing age assignments of unconformities, sedimentary interruptions, sedimentary turnovers, and onset of drift deposition 3. Reconstruct and date bank to drift turnover
Drilling program:	Hole A: APC to 80 mbsf. Hole B: drill/wash to 80 mbsf, RCB to 1060 mbsf
Logging and downhole measurement program:	Wireline log with triple combo and FMS-sonic.
Nature of rock anticipated:	Calcareous ooze, chalk, limestone

Site KK-03B

Priority:	Primary
Position:	15.034617°N, 71.026561°N
Jurisdiction:	India
Water depth (m):	2400
Target drilling depth (mbsf):	450
Approved maximum penetration (mbsf):	900
Survey coverage (track map; seismic profile):	Location map (Fig. F10) Primary line(s): Lines K-95-51A-II and K-95-8B (Fig. F11)
Objective(s):	1. Reconstruction of oceanic and terrestrial monsoonal paleoclimate in the Arabian Sea and Indian Peninsula since the Oligocene 2. Reconstruction of oceanic and terrestrial premonsoonal paleoclimate in the Arabian Sea and Indian Peninsula in the Eocene and upper Paleocene
Drilling program:	Triple APC to 200 mbsf Double XCB to 450 mbsf
Logging and downhole measurement program:	No logging program
Nature of rock anticipated:	Nannofossil and foraminifer oozes

Site summaries (continued)

Site KK-03A

Priority:	Alternate
Position:	15.3061°N, 70.9032°E
Jurisdiction:	India
Water depth (m):	2685
Target drilling depth (mbsf):	450
Approved maximum penetration (mbsf):	900
Survey coverage (track map; seismic profile):	Location map (Fig. F10) Primary line(s): Line K-95-8B (Fig. F11)
Objective(s):	1. Reconstruction of oceanic and terrestrial monsoonal paleoclimate in the Arabian Sea and Indian Peninsula since the Oligocene 2. Reconstruction of oceanic and terrestrial premonsoonal paleoclimate in the Arabian Sea and Indian Peninsula in the Eocene and upper Paleocene
Drilling program:	Triple APC to 200 mbsf Double XCB to 450 mbsf
Logging and downhole measurement program:	No logging program
Nature of rock anticipated:	Nannofossil and foraminiferal oozes

Expedition scientists and scientific participants

The current list of participants for Expedition 359 can be found at **iodp.tamu.edu/scienceops/expeditions/maldives_monsoon.html.**